Discover Sustainability

https://doi.org/10.1007/s43621-026-03902-6

Article in Press

A comprehensive review of nanocatalysts for sustainable plastic waste valorization in circular economy

Received: 17 March 2026

Accepted: 15 June 2026

Published online: 27 June 2026

Cite this article as: Padmanabhan S., Alsayaydeh J.A.J., Kumar T.V. *et al.* A comprehensive review of nanocatalysts for sustainable plastic waste valorization in circular economy. *Discov Sustain* (2026). https://doi.org/10.1007/s43621-026-03902-6

S. Padmanabhan, Jamil Abedalrahim Jamil Alsayaydeh, T. Vinod Kumar, S. Ganesan, Rex Bacarra & Nadzrie Bin Mohamood

A Comprehensive Review of Nanocatalysts for Sustainable Plastic Waste Valorization in Circular Economy

S. Padmanabhan[1], Jamil Abedalrahim Jamil Alsayaydeh[2*], T. Vinod Kumar[3*], S. Ganesan[4], Rex Bacarra[5], Nadzrie Bin Mohamood[2]

[1]Department of Mechanical Engineering, Vel Tech Rangarajan Dr.Sagunthala R&D Institute of Science and Technology, Chennai, India, padmanabhan.ks@gmail.com
[2]Department of Engineering Technology, Fakulti Teknologi Dan Kejuruteraan Elektronik Dan Komputer (FTKEK), Universiti Teknikal Malaysia Melaka (UTeM), 76100 Melaka, Malaysia, jamil@utem.edu.my, nadzrie@utem.edu.my
[3]Department of Mechanical Engineering, Vels Institute of Science, Technology and Advanced Studies (VISTAS), Chennai, India, vinod.se@vistas.ac.in
[4]Department of Mechanical Engineering, Sathyabama Institute of Science and Technology, Chennai, India, ganesan.mech@sarhyabama.ac.in
[5]Department of General Education and Foundation, Rabdan Academy, Abu Dhabi, United Arab Emirates. rbacarra@ra.ac.ae
[*] Corresponding author: jamil@utem.edu.my AND vinod.se@vistas.ac.in

ABSTRACT

The rapidly growing amount of plastic waste has become one of the most difficult environmental problems that humanity will have to face in the 21st century. Nano-engineered catalysts have emerged as a technically promising approach. These offer systematic benefits over bulk catalytic materials because of the higher surface-to-volume ratios, programmable acid–base surface chemistry and morphology-dependent active site exposure. This review critically evaluates the mechanistic basis, material-specific performance and practical limitations of four major nanocatalyst types, namely metal oxide nanoparticles, magnetic nanocatalysts, nano-zeolites and hybrid nanocomposites, in thermo-chemical plastic conversion, focusing on catalytic pyrolysis. Under optimised laboratory settings and clean single polymer feeds, nano-catalytic systems achieve plastic-to-liquid conversion efficiencies of 75-92 wt% with fuel calorific values of 43-46 MJ/kg significant gains over uncatalyzed thermal pyrolysis. These statistics, however, are for ideal situations and performance is often 15–25% lower with post-consumer mixed plastic feeds. This review critically discusses deactivation mechanisms such as coking, sintering and chemical poisoning, multi-cycle stability constraints, nanotoxicological risk and economic feasibility at industrial scale features seldom covered in the literature. Life cycle assessment evidence indicates net greenhouse gas savings of 1.2–2.8 kg CO_2 equivalent per kilogram of plastic treated, but this range is quite sensitive to system boundary assumptions, grid carbon intensity and catalyst recovery efficiency.

Keywords: *Nanocatalysts, Plastic waste pyrolysis, Waste-to-fuel conversion, Thermochemical valorization, Circular economy, Metal oxide nanoparticles*

1. INTRODUCTION

Global production of synthetic plastics has increased dramatically since the mid-twentieth century, reaching over 400 million tonnes annually by 2023. However, less than 10% of all plastic waste accumulated over time has been recycled (Geyer et al., 2026). The rest remains in landfills, terrestrial ecosystems, and marine environments. When plastic chemically breaks down, it actually gets stronger. This is the same feature that makes plastic commercially valuable. Characteristics that make plastic a valuable commodity are also those that make it highly durable and hence one of the most persistent pollutants in the environment. Mechanical recycling, incineration, and landfilling which are conventional waste management methods,

are hardly capable of solving the worldwide plastic waste problem due to its massive scale, diversity, and chemical complexity. This led to a significant demand for new technologies for the treatment of plastic waste that can recover plastic waste chemical energy and material values at the waste's end of life (Al-Salem et al., 2009; Qureshi et al., 2020).

Thermochemical conversion, and pyrolysis in particular, is one of the techniques that has emerged as one of the most effective ways for plastic waste valorization. Using this method mixed contaminated, and non-recyclable plastic wastes can be converted into liquid hydrocarbon fuels, combustible gases, and carbonaceous materials (Panda et al., 2010). However, thermal pyrolysis untreated is associated with a number of drawbacks such as high energy consumption, formation of much diversified products that are difficult to control, and considerable generation of solid residues. These drawbacks were majorly responsible for this method being less economically competitive than fossil fuel-based alternatives. Introducing catalysts into the pyrolysis processes has been proven an effective way of solving the above-mentioned problems. Catalysts are crucial in reducing the activation energies, directing the product composition to be more like gasoline and diesel hydrocarbons, and reducing the formation of char and coke that are generally not desirable (Miandad et al., 2016; Williams & Slaney, 2007). On the one hand, research has shown that conventional zeolites and alumina-based materials are two groups of catalysts that have been able to present significant performance benefits. On the other hand, these materials are characterized by having relatively low external surface areas as well as significant intraparticle diffusion resistances. Due to these inherent properties, they not only limit the extent to which conversion efficiency can be maximized but also impose kinetic ceilings on the quality of the products that can be obtained (Serrano et al., 2012). Nanotechnology can revolutionize the field by enabling the design of catalytic materials that are perfectly controlled in terms of particle size shape crystal structure, and surface chemistry, all at the nanoscale level. The combination of these features results in an incredible increase in catalytic activity, selectivity, and stability compared to conventional bulk materials (Alreshidi et al., 2025; Serrano et al., 2012). Metal oxide nanoparticles, magnetic nano catalysts, nano-zeolites, and hybrid nano composites each one has been effectively used in plastic pyrolysis. Yet, the research is still scattered in individual material studies without a unifying, critical synthesis of structure activity relationships, process integration considerations, and waste-to-wealth potential (Anuar Sharuddin et al., 2016). Literature comparison of this review with recently published review articles are listed below:

Aspect	(Azam et al., 2024)	(Wei et al., 2025)	(Hijazi et al., 2025)	(Shi et al., 2025)	(Hashemi et al., 2026)
Nanocatalyst Focus	Hierarchical zeolites for hydrocracking	Zeolite catalysts for heavy oil cracking	Zeolite transport limitations	Mixed plastic catalytic recycling	Advanced pyrolysis for mixed plastics
Plastic-Specific Degradation Pathways	Partial	Not addressed	Not addressed	Partial	Partial
Catalyst Deactivation	Limited	Limited	Moderate	Moderate	Limited
Circular Economy Integration	Not addressed	Not addressed	Not addressed	Partial	Not addressed
Nanotoxicity & Health Risks	Not addressed	Not addressed	Not addressed	Not addressed	Not addressed

Despite the expanding body of literature on catalytic plastic valorization, current reviews do not collectively offer a unified treatment of nano-specific structure-activity relationships across all major catalyst classes, plastic-type-specific degradation pathway mapping, and critical discussion of catalyst deactivation mechanisms. Furthermore, no previous research has concurrently considered nanotoxicity and environmental health hazards of nanomaterials, economic feasibility at industrial scale and circular economy integration in one holistic framework. This review is thus explicitly meant to fill these identified gaps, delivering a critical, balanced and mechanistically grounded synthesis of nanocatalytic plastic waste valorization.

Although other literature on nano-catalytic plastic valorisation is emerging, reviews on this area are to some extent limited. Comprehensive reviews on catalytic pyrolysis (Anuar Sharuddin et al., 2016; Miandad et al., 2016) overlook nanoscale structure–activity relationships, reviews on advanced catalysts for polyolefins (Serrano et al., 2012) neglect reactor engineering, economic feasibility and environmental risk assessment, and the latest review on nanocatalysts (Alreshidi et al., 2025) does not discuss catalyst deactivation mechanisms, multi-cycle stability and nanotoxicology. No existing review simultaneously addresses the following points: (i) nano-surface chemistry directly relevant to the molecular structure of each type of plastic (PE, PP, PVC, PET, PS), (ii) critical comparative performance assessment of metal oxide nanoparticles, magnetic nanocatalysts, nano-zeolites, and hybrid nanocomposites, (iii) reactor engineering and scale-up evaluation for nanocatalyst applications, (iv) balanced assessment of deactivation, regeneration and multi-cycle stability in realistic conditions, (v) techno-economic feasibility and industrial scalability evaluation, and (vi) nanotoxicological and life cycle environmental risk assessment. The present review fills this gap in a comprehensive way. It details the mechanistic rules that govern nano-catalytic polymer degradation, assesses the catalytic performance of different materials in different feedstocks and operating conditions, investigates reactor designs and their potential for nanocatalyst application at scale, and critically assesses the limitations, environmental risks, and economic circumstances that determine whether nano-catalytic plastic valorisation is and is not a viable industrial option.

2. NANO-CATALYSIS IN POLYMER DEGRADATION: MECHANISMS AND PRINCIPLES

This section lays out the basic mechanistic foundations of nanocatalyst behavior in polymer degradation: the surface chemistries promoting chain scission, the structure parameters controlling activity, and the relative performance benefits of nanomaterials relative to traditional bulk catalysts.

2.1 Nano-Surface Chemistry and Polymer Chain Scission

The thermochemical transformation of synthetic polymers is predicated upon the stable interaction of catalyst active sites with polymeric chain segments (Figure 1). Confinement effects in nanocatalysts mean they have physico-chemical characteristics that radically differ from traditional bulk catalysts including amplified surface-to-volume ratios and surface atoms that are coordinately unsaturated (Anuar Sharuddin et al. 2016). These properties help nanocatalysts to protract polymer chain scission at far lower temperatures than those present in uncatalysed thermal cracking.

2.1.1 Mechanistic role of Bronsted and Lewis acid sites

The surface chemistry of nanocatalysts in polymer cracking takes place with two main acidbase pathways. Proton transfer from Bronsted acid sites to the polymer backbone generates

carbocation-type species that promote β-scission of C–C bonds. Lewis acid sites electron deficient metal atom sites that act as electron pair acceptors coordinate to electron dense sites within the polymer chain, weakening the C-C and C-H bonds and Because of this enhancing bond cleavage. Because of a nanocatalysts high surface to volume ratio, they expose valuable acid sites in much higher concentrations per weight than traditional size catalysts, leading to a much higher catalytic turnovers (Miandad et al. 2016).

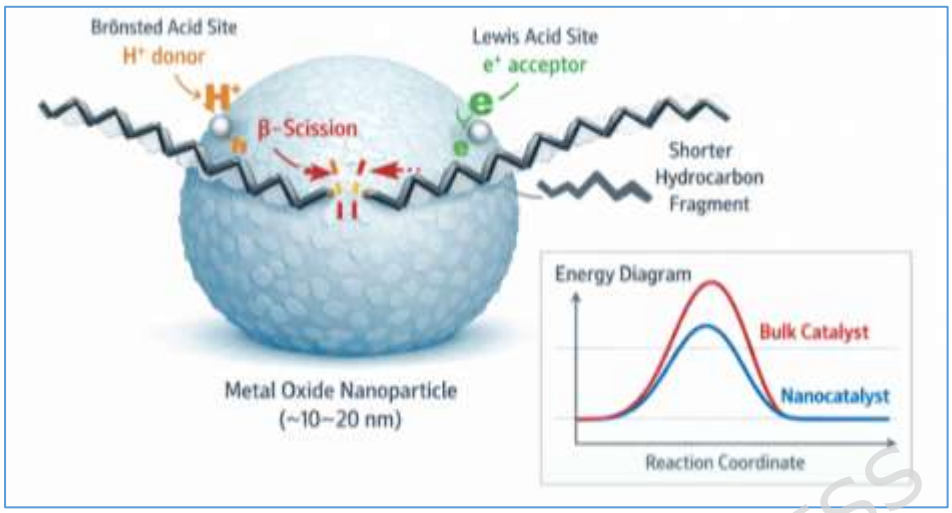

Figure 1: Nano-Surface Chemistry and Active Site Mechanisms in Polymer Chain Scission

A key aspects of nanocatalyst surfaces is the confinement in space of polymer chain segments at or within the catalyst structure, whereby PE and PP chains intimately connected to nanoparticle surfaces exhibit heightened local concentrations of reactive chain ends at active sites, thereby minimizing diffusion barriers to access and allowing kinetically facile access to the scissile C-C bonds (Lopez et al. 2017). Morales Pacheco et al. found nanoscale ZSM-5zeolites (< 100 nm) to lower the activation barrier for PE cracking between 30 and 45 kJ/mol relative to more conventional ZSM-5zeolites of the same composition, a consequence of increased surface accessibility, and number of acid sites exposed to the polymer (Broclawik et al. 2011).

2.1.2 Surface chemistry and polymer-specific degradation

An important consideration unnoticed in general discussions of acid-base catalysis, which is essential for understanding the acid-base catalysis involved in polymer degradation. The degradation pathway of a polymer significantly depends on the specific forms of its molecular structure.

Table 1. Plastic type, degradation pathway, and preferred nanocatalyst surface chemistry

Plastic type	Key structural feature	Primary degradation pathway	Preferred surface chemistry	Example nanocatalyst
Polyethylene (PE)	Long unbranched alkyl chains	Random-scission carbocation chain cracking	Strong Bronsted + Lewis acidity	Nano-ZSM-5, γ-Al_2O_3 NPs
Polypropylene (PP)	Tertiary C–H at every repeat unit	Preferential β-scission at tertiary carbons	Lewis acidity targeting tertiary C	TiO_2 (anatase) NPs, nano-ZSM-5
Polystyrene (PS)	Phenyl groups; prone to depolymerization	Radical chain unzipping → styrene monomer	Mild acidity; radical initiation sites	Fe_3O_4 NPs, ZnO NPs
PVC	C–Cl bonds; HCl evolution below 300°C	Two-stage: dechlorination then cracking	Strong Basicity for HCl scavenging	MgO NPs (base catalyst)
PET	Ester linkages; aromatic rings	Ester hydrolysis/pyrolysis → benzoic acid, CO_2	Lewis acidity + redox sites	TiO_2–Fe doped NPs

NPs = nanoparticles; PE = polyethylene; PP = polypropylene; PS = polystyrene; PVC = polyvinyl chloride; PET = polyethylene terephthalate.

Due to the variety of plastic types, structurally differing problems arise that lead to different favored chemistries on a catalyst surface. This is tabulated in table 1. For polyolefins (PE, PP) the cracking occurs by a carbocationic mechanism, at the Brnsted acid sites, which involves more random chain scission, resulting in a wide distribution of hydrocarbons that are readjusted by the catalyst pore structure and acid strength (Verma et al. 2017). For PP in particular, In reality in every repeat unit there are tertiary carbons makes this polymer more active for Lewis acid activation: Ti^{4+} in anatase TiO_2 selectively adsorbs at tertiary C-H bonds, and scission is thereby directed at C_3–C_5 olefins with 63% selectivity, for example (Verma et al. 2017).

Degradation of PVC presents a fundamentally different problem. Its primary degradation step (150–300°C) is a dehydrochlorination a strongly basic elimination of HCl, which must be controlled as to avoid promoting the formation of chlorinated aromatic byproducts (dioxins, furans) in the subsequent high temperature cracking stage. MgO nanocubes a model material for a strongly basic surface sufficient acidity to re-abstract the HCl and prevent aromaticity from dominating the product cluster distribution while assisting in stabilization of surface bound chloride as Cl (Luo et al. 2000). Strong Bronsted acidity is precisely what makes nano-ZSM-5 catalytically very active for PE cracking it would be detrimental with PVC as it would promote dioxin formation rather than scavenge it.

Further complexity is added in PET degradation by its additional decarboxylation with ester linkage hydrolysis, which in turn yields CO_2 and oxygenated products. Bifunctional nanocatalysts able to combine a Lewis acid site (needed for activating the ester carbons) with a moderate redox activity (required to achieve decarboxylation and deoxygenation) are crucial for this process. Fe doped TiO_2 nanocrystals, for example, are able to modify the distribution of products from predominantly oxygenated species toward meaningful C_8–C_{10} aromatic cuts, both optimizing fuel value and carbon usage (Antelava et al. 2019).

2.1.3 Thermal conductivity and heat transfer at the nanoscale

Apart from its surface chemistry, metallic and metal oxide nanoparticles display thermal conductivities (approaching 350 W/m.k) that are much superior to those of typical bulk ceramic catalyst, facilitating quick and even heating of the polymer melt stage during pyrolysis while limiting the thermal gradients of the reactor bed that during conventional packed beds system lead to site-specific melting, That means to the unwanted production of solid char and coke

deposit. This results in having a narrower product spectrum as well as a lower amount of residual solids, a consequence of having energy-efficient control of chain scission that have been repeatedly presented in nano-catalytic systems (Sharuddin et al. 2018).

2.2 Size and Morphology Effects on Catalytic Activity

Catalyst efficiency depends on the chemical composition of nanostructures and as defined by the particle size, surface morphology, and crystallographic phase (structural parameters), which influence the type, amount, and accessibility of the active surface sites (Singh et al. 2019). Such structure activity relationships are crucial for the rational design of superior nanocatalysts for plastic waste conversion.

2.2.1 Particle size scaling

As particle size is scaled down from micrometers to nanometers, the fraction of atoms on the surface of the particle increases rapidly, with a 10nm diameter cluster exhibiting approximately 20% surface atoms, and a 1nm cluster essentially 100% surface exposed. This translates directly into increased catalytic performance more accessible active sites per gram of catalyst means higher turn-over frequencies and a higher conversion per gram of catalyst (Alreshidi et al. 2025). For acid-functionalized metal oxide nanocatalysts used in polyolefin pyrolysis, this size effect was quantified as oil-yield increases of between 15 and 40% over their micron-scale equivalents in pyrolisis experiments conducted under otherwise identical conditions. (Sarker & Rashid, 2013).

Figure 2: Size and Morphology Effects of Nanoparticles on Catalytic Activity

Ratnasari et al. as a rigorous quantitative demonstration, reported that 8 nm mean particle size γ-Al_2O_3 Nano-catalyst produced 78.4 wt% liquid oil (from LDPE pyrolysis at 450°C) versus 61.2 wt% using a commercial Al_2O_3 (mean particle size 2.3 µm). This 28% excess liquid yield is the result of synergic effects from nano-size, phase composition, and surface acid site density (Ratnasari et al. 2017). Such substrate-species effects held true across catalyst families and feedstocks as tabulated in Table 2.

Table 2. Effect of Nanoparticle Size and Morphology on Catalytic Pyrolysis Oil Yield from Plastic Waste

Catalyst	Particle Size (nm)	Morphology	Plastic Feed	Temp. (°C)	Oil Yield (wt%)	Key Observation	Reference
γ-Al_2O_3 NPs	8	Spherical	LDPE	450	78.4	28% yield gain vs. bulk Al_2O_3	(Ratnasari et al., 2017)
ZSM-5 Nano-zeolite	<100	Cubic	PE	500	82.1	Lower activation energy by ~40 kJ/mol	(Broclawik et al., 2011)
TiO_2 Nanosheets	15–20	2D sheet (001 facet)	PP	430	74.6	High Lewis acidity from exposed facets	(Zhang et al., 2016)
MgO Nanocubes	20–30	Cubic (100 facet)	Mixed plastic	480	69.3	Base-catalyzed elimination of PVC	(Onwudili et al., 2009)
ZnO Nanorods	40–60	Rod	HDPE	460	71.8	Shape-selective cracking; low char	(Zhang et al., 2016)
Fe_3O_4 Nanospheres	10–15	Spherical	PS	420	68.5	Magnetic recovery; stable over 5 cycles	(Ali & Siddiqui, 2005)

NPs = nanoparticles; PE = polyethylene; PP = polypropylene; HDPE = high-density polyethylene; PS = polystyrene; PVC = polyvinyl chloride; LDPE = low-density polyethylene.

2.2.2 Morphology and crystallographic facet exposure

Particle shape defines the selection of crystallographic facets exposed at the particle surface and well known to possess unique electronic and acidbase properties. Anatase TiO_2 nanosheets which are modified to contain predominantly high-energy (001) facets possess a stronger Lewis acidity than spherical anatase particles which are of the same phase and size because the (001) surface exposes a greater number of coordinatively-unsaturated Ti^{4+} sites (Zhang et al. 2016). Also, MgO nanocubes that are mainly enclosed by (100) facet surfaces comprising Mg^{2+}–O^{2-} ion pairs possess an enhancement in surface basicity over MgO nanospheres of the same phase and size a facet-dependent effect which Because of this improves HCl removal efficacy in PVC degradation (Onwudili et al. 2009). ZnO nanorods exhibit a shape-dependent inhibition in char formation during cracking studies compared to spherical ZnO samples under similar conditions which is ascribed to the anisotropic distribution of prismatic (1010) facets (Zhang et al. 2016).

2.2.3 Crystal phase effects

Crystal structure and phase composition is another facet of structural control. The active γ-phase of Al_2O_3 can be stabilized at grain sizes of less than ~ 10 nm, giving a defect spinel structure with the penta-coordinated Lewis acidic surface sites of aluminum that are thermally stable, rather than the thermodynamically accessible and inactive α-phase (Yahaya et al. 2013). Anatase TiO_2 (metastable at below 600°C) will have a surface area of 80–200 m^2/g and a Lewis acidity that persists at higher values than rutile TiO_2, although all the anatase will tend to convert to rutile above 600°C (Yahaya et al. 2013).

2.3 Nano-Engineered vs. Conventional Catalysts: Quantitative Comparison

The mechanistic benefits discussed in the previous subsections, because of this lead to systematic and quantifiable performance discrepancies when nano-engineered catalysts are benchmarked versus canonical catalytic materials bulk zeolites, amorphous silica alumina and commercial alumina across several performance indicators (Miandad et al. 2016; Sharuddin et al. 2018). Traditional catalysis materials such as FCC zeolites, H-ZSM-5 in their conventional micrometric form are characterized by well-known Bronsted acidity and shape selective architecture, But their low external surface areas (10–50 m^2/g for FCC type) coupled with relatively large intraparticle diffusion resistances impose kinetic limitations on the catalytic

conversion of very large polymer molecules which are unable to reach the zeolite interior (Qureshi et al. 2020). Nano-engineered zeolites with crystal sizes ranging from 30-100 nm exhibit high external surface areas in the range of 100–400 m^2/g an increase of 5-10 across the different catalysts greatly reducing diffusion pathways and enabling far more acid sites to be utilized (Broclawik et al. 2011).

Catalyst loading factors also favor nanosystems. The apparent specific activity of nanocatalysts supports the conversion of plastic at catalyst:plastic ratios of 1:10 to 1:20 by weight, versus 1:3 to 1:5 for the conversion of conventional catalysts to attain similar conversion levels. Abbas-Abadi et al. demonstrated this experimentally: nano-ZSM-5 was able to attain 89.3%HDPE conversion to liquid hydrocarbons at 500C with a dosage of 5wt%, versus 20 wt% ZSM-5 to recover an 85.7% conversion (Abbas-Abadi et al. 2014).

This four times reduction in catalyst usage would reduce operating costs, reduce the amount of catalysts requiring regeneration, and lessen the net amounts of spent catalyst. Product selectivity enhancement is perhaps of most direct Commercial value. Typical acid catalysts produce a broad product distribution of C_1–C_{30}^+ hydrocarbons, with significant proportions of low value gases in the light ends (C_1–C_4) and heavy waxes at the heavy end. Nano-engineered catalysts with strongly control of pore geometries, on-demand optimization of acid strength and chemistry, and from robust, chemically resistant material scan channel cleavage events to favor the C_5–C_{12} gasoline range and C_9–C_{16} kerosene range, generating liquid fuels with a heating value of 42 -46MJ/kg comparable to established petroleum products (Ratnasari et al. 2017; Sarker & Rashid, 2013). The key quantitative impacts by catalyst class are summarized in Table 3.

Table 3. Comparative Performance of Conventional vs. Nano-Engineered Catalysts in Plastic Pyrolysis

Parameter	Conventional Catalysts	Nano-Engineered Catalysts	Improvement Factor
BET Surface Area (m^2/g)	100–300	200–800	2–4×
External Surface Area (m^2/g)	10–50	100–400	5–10×
Acid Site Density (μmol/g)	200–600	500–1500	2–3×
Catalyst Loading (wt%)	15–25	3–8	70–80% reduction
Liquid Oil Yield (wt%)	55–70	70–90	15–30% gain
C_5–C_{12} Selectivity (%)	35–55	55–80	20–40% gain
Activation Energy (kJ/mol)	180–250	120–190	25–35% reduction
Coke Formation (wt%)	5–15	1–6	50–80% reduction
Catalyst Reusability (cycles)†	3–5	5–10	2× improvement

†Catalyst reusability numbers are indicative of performance in optimised lab circumstances with virgin single-polymer feeds and sonication-assisted solvent wash between cycles—regeneration technique not readily scalable to industrial operation. Industrial calcination regeneration has a sintering penalty of 3–8% surface area loss each cycle and mixed post-consumer plastic feeds are predicted to have feasible cycle counts 30–50% lower than the laboratory values described here. Moreover, the lack of standardised regeneration techniques in the literature prevents the cross-study comparability of reusability data.

3. NANOMATERIALS FOR WASTE-TO-FUEL CONVERSION: MATERIAL-SPECIFIC PERFORMANCE

The preceding section established the mechanistic and structural principles governing nanocatalyst action. This section evaluates the four principal classes of nano-engineered catalysts metal oxide nanoparticles, magnetic nanocatalysts, nano-zeolites, and hybrid nanocomposites focusing on their material-specific catalytic performance, selectivity profiles, and operational characteristics in plastic waste conversion.

3.1 Metal Oxide Nanoparticles

Metal oxide based catalysts are arguably the most-studied class of catalyst for thermochemical plastics conversion due to their adjustable surface acid/base behavior, high thermal stability and modest synthesis cost. The fundamentals of surface chemistry on metal oxides that influence the reactions Lewis and Bronsted acidbase character, interaction with the specific facets of a given morphology, and dependence on the plastics typeare discussed earlier; the unique performance aspects of each metal oxide system are discussed below:

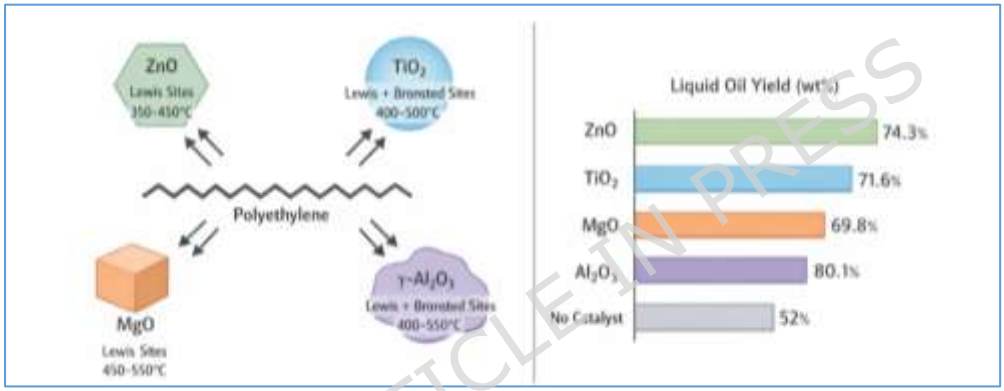

Figure 3: Metal Oxide Nanocatalyst Mechanisms and Product Distribution in Plastic Pyrolysis

3.1.1 ZnO nanoparticles

ZnO nanoparticles (NPs) in the wurtzite crystal phase possess surface oxygen vacancies in the Zno lattice that act as Lewis acid sites that can activate C-H and C-C bonds in the polyolefin chains (Maqsood et al. 2021). When used in the temperature range of 400-500C, ZnO NPs (15-40 nm) selectively produce aromatic and olefinic hydrocarbons (**C_6–C_{12})** on polyethylene and polystyrene feeds. The Lewis acidity was further enhanced by reducing particle size below 20 nm as this increased the surface/bulk ratio of oxygen vacancies providing an increased number of coordinatively unsaturated zinccenters (Maqsood et al. 2021). Demirbas also used ZnO NPs at 10 wt% to produce a liquid oil yield of 74.3 wt% in the pyrolysis of co-mixed polyolefin waste at 450°C. These NPs produced a higher **C_8–C_{12}** range fraction of the liquid product at 52% total yield relative to conventional thermal pyrolysis with no catalyst was used at around 18% (Demirbas, 2004). ZnO remains in the catalytically active wurtzite form until 600°C at which point it reduces to catalytically inactive metallic zinc. An important drawback of using ZnO nanoparticles in feeds containing blended plastics is that it is very sensitive towards co-polymers with chlorine: surface Zn^{2+} sites easily generate stable $ZnCl_2$ compounds from the HCl gas released by PVC cracking, resulting in the poisoning of the catalyst. In reality, it is recommended to use ZnO nanocatalysts in polyolefin and ps feed stocks; when such catalysts

are used in feeds with PVC streams, then the latter has to be washed out beforehand or to use an additional basic scavenger MgO.

3.1.2 TiO_2 nanoparticles

Anatase TiO_2 nanoparticles (10-25 nm) provide a combination of Lewis acidity, photocatalytic activity, and thermal stability below between 300 and 550°C, where the anatase-to-rutile phase transformation destroys surface area through grain growth. At 300-550°C, anatase TiO_2 selectively catalyzed Lewis acid-catalyzed cracking of PP and PET. During PP cracking at 450°C, nanoscale anatase TiO_2 directed 63% of the total carbon products to C_3–C_5 olefins due to the increased adsorption of tertiary PP carbons at Ti^{4+} Lewis sites (Verma et al. 2017). Doping with transition metals (Fe, Ni) makes TiO_2 a bifunctional acid-redox catalyst that enables simultaneous cracking and mild hydrogenation of unsaturated product (a key improvement for the chemical stability and storage of the resulting liquid fuel; Antelava et al. 2019).

3.1.3 MgO nanoparticles

Unlike the preceding metal oxides, MgO is required as a catalyst based on weakly basic, unlike acidic action (Section 2.1.2). Its utility is That means in the two-stage handling of chlorinated plastics (a) base-catalyzed HCl removal from PVC in the range 150-300°C, sequestering released chlorine before it can be incorporated into dioxins and furans, and (b) thereafter base-promoted cracking of the dechlorinated polymer at 380-480°C, resulting in alkene present distribution via a carbanion pathway. MgO nanoparticles (particle size 20-50 nm)as used by Luo et al. reduced the activation energy of LDPE degradation by 38 kJ/mol compared to the uncatalyzed process (Luo et al. 2000). The high melting point of MgO (2852°C) promotes stability through the practical pyrolysis range.

3.1.4 γ-Al_2O_3 nanoparticles

Among the metal oxide nanocatalysts, γ -Al_2O_3 nanoparticles have been studied most extensively for plastic pyrolysis, due to their well-defined surface acidity consisting of penta-coordinated Al^{3+} Lewis sites and surface hydroxyl Bronsted sites, excellent thermal stability to about 850°C, and commercial availability. A two-site cracking mechanism of Lewis site adsorption/activation followed by Brønsted-assisted fragmentation is described in Section 2.1.1. Aguado et al. quantitated particle size effects on yield at 500°C in a systematic comparative study, and found that, compared to bulk Al_2O_3 (2.5 μm), nano-sized (8 nm) and mesoporous (50 nm) Al_2O_3 resulted in approximately 80.1, 71.4, and 58.9 wt% HDPE liquid oil yield, respectively. However, the 8 nm nanoparticles also resulted in the highest liquid oil yield of C_5–C_{12}, with 64 wt% of the liquid produced. A summary of key metal oxide nanocatalyst performance metrics is presented in Table 4.

Table 4. Comparative Performance of Metal Oxide Nanocatalysts in Plastic Pyrolysis

Catalyst	Size (nm)	Surface Area (m^2/g)	Plastic Feed	Temp. (°C)	Liquid Yield (wt%)	Dominant Product Range	Thermal Stability (°C)	Reference
ZnO NPs	15–40	30–80	Mixed polyolefins	450	74.3	C_8–C_{12} aromatics/olefins	Up to 600	(Demirbas, 2004)
TiO_2 (anatase) NPs	10–25	80–200	PP	450	71.6	C_3–C_5 olefins	Up to 550	(Verma et al., 2017)
MgO NPs	20–50	50–150	LDPE / PVC	420	69.8	Linear alkenes	>2000 (mp)	(Luo et al., 2000)
γ-Al_2O_3 NPs	8–15	200–400	HDPE	500	80.1	C_5–C_{12} gasoline range	Up to 850	(Mollick et al., 2025)
ZnO–Al_2O_3 composite	20–35	150–250	LLDPE	470	76.8	C_6–C_{14} mixed	Up to 700	(Antelava et al., 2019)
TiO_2–Fe (doped)	12–20	120–180	PET	480	65.2	C_8–C_{10} aromatics	Up to 600	(Antelava et al., 2019)

NPs = nanoparticles; PP = polypropylene; LDPE = low-density polyethylene; HDPE = high-density polyethylene; LLDPE = linear low-density polyethylene; PET = polyethylene terephthalate; PVC = polyvinyl chloride.

The reported range of liquid yields for γ-Al_2O_3 nanocatalysts (61–80 wt%) is wider than would be expected based on compositional variations alone. The principal sources of discrepancy are particle size (8 nm vs. 50 nm specimens giving 9 percentage points yield difference under identical conditions; Aguado et al., 2007), reactor configuration (fluidized-bed exceeding fixed-bed by 8–12 percentage points at equivalent loading; Obeid et al., 2014), and feed composition (virgin HDPE vs. post-consumer mixed polyolefins differing in high-molecular-weight chain content, which most benefits from nano-surface accessibility). Studies showing yields in the lower half of this range invariably use larger particles in fixed-bed arrangements with post-consumer feeds circumstances that collectively decrease intrinsic nano-activity regardless of catalyst composition.

3.1.5 Comparative synthesis: selectivity–yield trade-offs across metal oxide nanocatalysts

The combined four metal oxide nanocatalyst systems show a consistent structure-selectivity relationship, where the main surface site (Lewis acidic, Bronsted acidic or basic) dictates activity, carbon chain length distribution, and the chemical class of the liquid product, irrespective of operating temperature or catalyst loading. This contrast is summarised in Table 5 for both metal oxide- and zeolite-based systems.

Both ZnO and TiO_2 are Lewis acid catalysts, but the product distributions are very different: ZnO produces C_8–C_{12} aromatics and olefins from polyethylene and TiO_2 produces C_3–C_5 olefins from polypropylene. This is attributed to facet-specific differences in substrate interaction; ZnO's oxygen-vacancy Zn^{2+} sites promote π-system formation and ring closure, whereas TiO_2's Ti^{4+} sites on (001) facets preferentially activate tertiary C–H bonds in the PP backbone, directing β-scission to short-chain olefins (Section 2.1.2). The choice of ZnO against TiO_2 is based on the product target and the molecular structure of the plastic feed and desired fuel percentage, not merely a matter of comparative activity.

γ-Al2O3 has the largest liquid oil yields of the metal oxide systems (80.1 wt % at 8 nm) and the broadest feedstock application, due to its dual Lewis–Bronsted feature. However, its gasoline-range product contains a higher percentage of linear alkanes than products from ZSM-5 catalysis, and so has lower octane ratings. This yield-octane tradeoff is repeated across catalyst classes. The most strongly shape-selective Brønsted acidity systems create the most

lucrative gasoline-range aromatics, but at the expense of rapid coking and narrower feedstock tolerance. MgO, however, occupies a very different niche – it is the only metal oxide acceptable for feeds containing PVC, where its basicity is a process need rather than a performance preference.

Reported liquid yields for ZnO nanoparticles are 68–78 wt% for polyolefin experiments, a range that cannot be explained by composition alone. Studies have shown greater yields with particle sizes below 25 nm in fluidised or well-mixed reactors based on the surface area and heat transfer principles. This heterogeneity highlights the need of documenting particle size, morphology and reactor type as standard information in catalytic pyrolysis articles, a far from ubiquitous practice in the existing literature (Table 5).

Table 5. Cross-catalyst comparison: surface character, selectivity, feedstock suitability, and mechanistic basis

Catalyst	Primary acid/base character	Dominant product range	Best-suited plastic	Key selectivity trade-off	Mechanistic basis
ZnO NPs	Lewis acid (O-vacancy Zn^{2+})	C_8–C_{12} aromatics/olefins	PE, PS	High aromaticity; Cl^- poisoning risk	O-vacancies favor π-system formation; wurtzite facets direct ring closure
TiO_2 (anatase) NPs	Lewis acid (Ti^{4+}, 001 facet)	C_3–C_5 olefins	PP, PET	High olefin yield; lower liquid fraction	Ti^{4+} activates tertiary C–H; β-scission bias toward short chains
MgO NPs	Strong base (O^{2-}, 100 facet)	Linear alkenes	PVC, LDPE	Good HCl scavenging; lower cracking rate	Carbanion mechanism; base sites neutralize HCl pre-dioxin stage
γ-Al_2O_3 NPs	Dual Lewis + mild Brønsted	C_5–C_{12} alkanes	HDPE, LLDPE	Broadest applicability; some wax carry-over	Two-step: Lewis adsorption then Brønsted proton fragmentation
Nano-ZSM-5	Strong Brønsted (shape-selective)	C_5–C_{11} aromatics + branched alkanes	PE, PP, mixed	Highest octane; narrowest feed tolerance	10-MR channels enforce C_5–C_{11} cut; secondary aromatization in pores
Ni/nano-ZSM-5	Brønsted acid + Ni^0 hydrogenation	C_5–C_{12} saturated hydrocarbons	Mixed PE/PP/PS	Best fuel stability; most complex synthesis	Bifunctional: zeolite cracks, Ni saturates olefins via H-transfer

NPs = nanoparticles; MR = membered ring; H-transfer = hydrogen transfer. Covers both metal oxide and zeolite systems for integrated comparison.

3.2 Magnetic Nanocatalysts for Efficient Recovery

Recovery and recycling of nanocatalysts is a practical imperative for economic feasibility at any scale of operation. The nanoscale particle size responsible for the high catalytic activity also presents a challenge for separation. Traditional means filtration centrifuging gravity settling require large amounts of energy, time, and ultimately result in imprecise recovery of nanoscale material (Rossi et al. 2014). Magnetic nanocatalysts circumvent this problem and can be rapidly separated and recovered in 90- 99% yields (Table 6) within minutes using an external magnetic field.

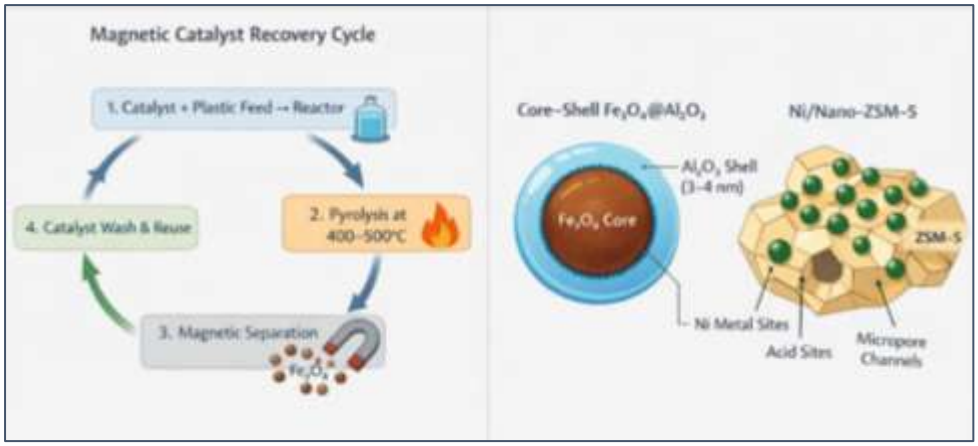

Figure 4: Magnetic Nanocatalyst Recovery Cycle and Nano-Zeolite Hybrid Architecture

3.2.1 Fe_3O_4 nanoparticles: superparamagnetic behavior and catalytic mechanism

When treated with an external magnetic field, superparamagnetic magnetite nanoparticles are strongly magnetized, and once the field is removed, they retain negligible remanent magnetization, making them resistant to aggregation when both stored or reused and subjected multiple times (Nguyen et al., 2021). The catalytic activity of magnetite in degrading polymers is attributed to Lewis-acidic sites that activate C–C bond cleavage via iron cations (Fe^{2+} or Fe^{3+}) on their surfaces, as well as through the creation of Fenton-type radicals to accelerate the rapid depolymerization of high-molecular-weight polyolefins by providing ionic and radical chain scission mechanisms through parallel pathways.

In one study, Sharuddin et al. investigated the use of 12 nm magnetite nanoparticles to catalyze the pyrolysis of high-density polyethylene (HDPE) at 450°C. They achieved a liquid oil yield of 68.5 wt% (i.e., 48% selectivity for kerosene-range hydrocarbons from C_{10} to C_{16}). The nanoparticles could be recovered by means of a 0.5 T neodymium magnet in 3 to 5 minutes per cycle. After washing in hexane, the magnetite nanoparticles retained 91.7% of their original activity across five cycles of use, significantly outperforming the typical 25% to 35% deactivation seen with non-magnetic nanocatalysts after mechanical separation. The cost of magnetite nanoparticles is estimated to be $15 to $30 per kilogram, and thus, magnetic recovery potentially allows for amortizing that cost over 8 to 10 cycles rather than 3 to 5 for non-magnetic catalytic systems, resulting in a reduction in average cost per cycle of approximately 60%.

Sharuddin et al. reported just 8.3% activity loss after five cycles, while previous Fe 3 O 4 investigations with similar particle size showed 15–22% deactivation after the same number of cycles . The main difference is in the regeneration protocol: sonication-assisted solvent washing recovers significantly more accessible surface area than simple immersion washing, as sonication breaks up carbonaceous deposits blocking the Lewis acid Fe sites without the need for high temperature calcination which could risk sintering. This procedural variable, infrequently reported as a primary experimental parameter, is likely to account for the majority of inter-study variation in Fe3O4 reusability data, and highlights the need for standardised regeneration protocols, prior to meaningful cross-study comparison of magnetic nanocatalyst longevity.

3.2.2 Core–shell architectures and spinel ferrite variants

Fe_3O_4 nanoparticles that have not been coated begin to transition from a default state to a catalytically inactive metallic iron state after achieving a temperature of 400 °C in a reducing

pyrolysis atmosphere. This conversion is the primary cause for uncoated magnetite deactivation. Core-shell configurations remedy this issue by coating a Fe_3O_4 core of ~10-15 nm in diameter with a thin shell (3-4 nm) of SiO_2, Al_2O_3 or ZSM-5 zeolite, thus providing chemical passivation of the iron oxide core while simultaneously creating a strong Brønsted acid surface to the outer shell (Nguyen et al., 2021). Nanda et al. demonstrated that a composite with a 12 nm magnetite core and 3-4 nm size alumina shell produced 75.2 wt% liquid oil from the pyrolysis of PP at 470 °C (10% more than a bare Fe_3O_4) while completely being recoverable magnetically and structurally stable after 7 cycles of reactions (Nanda et al, 2018).

Other spinel ferrites, such as $NiFe_2O_4$, $CoFe_2O_4$, and $MnFe_2O_4$, have also been studied as magnetic catalysts for the valorization of plastics. $NiFe_2O_4$ nanoparticles (15-25 nm) contain both surface Ni^{2+} and Fe^{3+} sites, providing them with a higher degree of Lewis acidity than Fe_3O_4. When used as catalysts for polystyrene pyrolysis, the $NiFe_2O_4$ produced a liquid yield of 72.4 wt% and enhanced the selectivity toward aromatics than that provided by bare Fe_3O_4. The saturation magnetization of these ferrites typically falls within the range of 30–80 emu/g, which makes them suitable for industrial-scale magnetic separation using permanent magnetic arrays to remove the catalyst from the effluent of the reactor without shutting down the process.

3.2.3 Synthesis: the activity–stability–recoverability trade-off

The literature on magnetic nanocatalysts as a whole demonstrates a three-way trade-off between catalytic activity, thermal stability and magnetic recoverability, which is not evident from individual studies of materials. The simplest recovery is with bare Fe3O4 NPs, however they tend to be reduced at temperatures above 400°C, losing both magnetic characteristics and catalytic activity. The core–shell structures (Fe_3O_4@Al_2O_3, Fe_3O_4@ZSM-5) are stable and add Brønsted acidity, but increase the complexity and cost of the synthesis. Spinel ferrites (NiFe2O4, CoFe2O4) exhibit higher Lewis acidity and better high temperature stability than Fe3O4, but lower saturation magnetisation (30–50 emu/g vs. 60–80 emu/g for Fe3O4), requiring larger magnetic fields for the same recovery efficiency at industrial scale. Notably, Sharuddin et al. reported an activity loss of 8.3% in five cycles for bare Fe3O4 while Nanda et al. (2018) found stability for seven cycles for core-shell Fe3O4@Al2O3, both under laboratory settings with clean polyolefin feeds. For mixed-plastic industrial feeds containing PVC, PET, or nitrogen-bearing polymers, much higher deactivation rates are expected because of surface poisoning by HCl, CO2 , and nitrogen species. None of the studies in the literature reviewed here have systematically assessed magnetic nanocatalyst deactivation under industrially relevant mixed-plastic feed compositions, a gap that must be overcome before magnetic catalyst recovery can be integrated reliably into industrial process designs.

3.2.4 Recovery Strategies for Non-Magnetic Nanocatalysts

The recovery of non-magnetic nanocatalysts such as ZnO, TiO2, gamma-Al2O3 and nano-zeolites remains a major engineering issue in nano-catalytic plastic pyrolysis. The most developed technology in terms of membrane filtration is ceramic membrane, which achieves 85–95% recovery for particles > 50 nm, although significant tar fouling causes the membrane flux to decrease by 40–70% in long-term operation. High-speed centrifugation can recover 75-90% of metal oxide nanoparticles but at a high energy input of 2-5 kWh/kg catalyst which is not economically feasible in large scale continuous operation.

The immobilisation of the catalyst on ceramic monoliths or metal foam supports avoids the need for post-reaction separation. Wash coated nano-zeolite and gamma-Al2O3 monoliths show stable activity despite a reduction of the available surface area by 20-40% due to diffusion

resistance. The other possibility is to embed in mesoporous matrices, e.g. SBA-15 silica, which prevents the agglomeration of the nanoparticles and ease the handling of traditional pellets. Encapsulated catalysts maintain 60-80% intrinsic surface accessibility and extend catalyst lifetime by 30-50%. Electrostatic precipitation shows up to 80-92% recovery of vapour phase nanoparticles at comparatively low energy consumption. But the effectiveness is limited by particle aggregation in hydrocarbon rich pyrolysis vapours . In summary, the immobilisation and encapsulation of the nanocatalysts are the most industrially viable methods for large scale applications of the non-magnetic nanocatalysts .

3.3 Nano-Zeolites and Hybrid Nanocomposites

The use of zeolite-based catalysts in acid-catalyzed hydrocarbon cracking has been at the core of FCC refineries for more than 60 years. Moving from traditional micrometre-sized crystals to novel zeolite nanostructures and metalzeolite hybrid nanocomposites offers the most dramatic step change in catalytic plastic valorization providing together or independently, increases in conversion, selectivity and stability (Serrano et al. 2012).

3.3.1 Nano-zeolites: transport regime transformation

Nano-zeolites are synthetic zeolite crystals with primary particle sizes in the 10-150 nm range, formed through hydrothermal crystallization with a structure directing agents, or by seeded crystal growth or confined mesoscale template synthesis (Serrano et al. 2003). The main performance benefit of grain size reduction to the nanoscale is a fundamental shift in the mass transport regime: while a typical commercial zeolite crystal (1-10 μm) needs intracrystalline diffusion of large polymeric fragments to access internal Brønsted acid sites to become rate limiting, nano-zeolites have shortened diffusion path lengths by 12 orders of magnitude to enable a far larger proportion of molecules to access structure acid sites per unit time (Hijazi et al. 2025).

ZSM-5 (an example of an MFI topology zeolite) has been the most common nano-zeolite used in catalytic cracking processes for plastics because of its intersecting channels formed from ten-member rings, where pore diameters are between 5.1 and 5.6 Å, and its ability to tune Brønsted acidity as measured by the Si/Al ratio. The production of liquid hydrocarbon fractions from polyolefin pyrolysis at 450 to 550 °C using nano-ZSM-5 crystals that are 50 to 100 nm in size generated liquid hydrocarbons that were greatly enriched in C_5-C_{11} aromatics and branched alkanes, which are high-octane components in gasoline. Gomis et al. demonstrated the impact of crystal size on LDPE catalytic pyrolysis at 500 ºC by comparing an 80 nm to 4 μm ZSM-5; the use of nano-ZSM-5 resulted in an increase in gasoline range liquid hydrocarbons (C_5-C_{12}) being produced from 41% to 67%, and a decrease in the amount of coke that was produced from 9.1 wt.% to 3.4 wt.%. These findings were attributed to less secondary cracking occurring as a result of the shorter diffusion channels and better shape-selective utilization of the micropores in the nano-ZSM-5 crystals (Gomis et al., 2007).

Beta zeolite (BEA topology) nanocrystals, which have a size of 20–80 nm, possess larger, 12-member ring, channels (6.4–7.6 Å) than the nano-ZSM-5 zeolite. These larger channels create less resistance to diffusion of larger polymer-derived particles into the Beta zeolite channels. Therefore, when cracking products are produced by the Beta zeolite, a much broader distribution of products is achieved into the C_{13}–C_{20} diesel range. The complementary cracking abilities between the Beta and ZSM-5 zeolites have led to the development of combinations of binary nano-zeolite mixtures and staged catalytic reaction configurations to produce customized multi-fraction fuel blends. Specifically, the broad capability of Beta for cracking

coupled with the selective shape-based cracking properties of ZSM-5 gasoline provides additional opportunities to customize multi-fraction fuel products.

3.3.2 Hybrid metal–zeolite nanocomposites

Hybrid metalzeolite nanocomposites are now leading the field in catalytic plastic recyclin, combining the acid cracking function of nanozeolites with the redox, hydrogenation or magnetic properties of transition metal nanoparticles in a single multifunctional catalyst. Catalyst architectures most commonly encountered involve depositing Ni Pd Mo or Fe nanoparticles (5-10 nm) on or within the walls of individual nano-zeolite crystals. These metal sites then increase the rates of hydrogen transfer reactions to saturate the olefinic and dieneic intermediatesthe major cracking productsfrom the zeolites, substantially reducing the unsaturation level of the liquid fuels produced and thereby improving their oxidative stability and combustion characteristics (Azam et al. 2024).

3.3.3 Synthesis: pore architecture, Si/Al ratio, and the selectivity–conversion relationship

Table 4 shows three trends for nano-zeolite and hybrid composite systems that are not explicitly clear from the description of the materials alone. Firstly, the liquid oil yield is related to the addition of a metal hydrogenation component: Ni/nano-ZSM-5 (84.7 wt%) is better than bare nano-ZSM-5 (82.1 wt%) not because of additional cracking but hydrogen transfer which converts reactive olefinic intermediates into stable saturated products before they undergo secondary cracking to light gases or condensation to coke. The metal component mainly affects fuel quality (calorific value 44.8 vs. 43.2 MJ/kg; olefin content 12% vs. 31%), not only yield increment.

Second, the selectivity for C_5–C_{12} scales with Si/Al ratio: lower ratios (greater acid site density) facilitate breaking outside of the gasoline range to light gases, while higher ratios reduce acidity and spatially concentrate products into the desired window. Si/Al ratios of 25-30 are consistently the best for a combination of liquid production and selectivity to the petrol range for all feedstocks. Below 15, extra coke is generated and over 50, activity is reduced to below economically usable levels. Third, the pore size defines the top cut-off in carbon number of the products. ZSM-5 (10-MR, 5.1-5.6 Å) imposes a shape selectivity, resulting in a C 11 -C 12 ceiling, while Beta zeolite (12-MR, 6.4-7.6 Å) allows for C 13 -C 20 products. Beta nanocrystals hence are more appropriate for diesel range fuel objectives. Despite the differences in yield and selectivity, the calorific values in Table 4 are impressively constant (42.9–44.8 MJ/kg), indicating a uniformly low heteroatom concentration for all systems. Therefore, the real-world discriminator for the systems is the stability of the fuel and the engine compliance rather than the energy content. These parameters are determined by the olefin content, aromatic distribution, and residual oxygen, all of which are in favour of the metal–zeolite hybrid composites as opposed to bare nano-zeolites.

The calorific value for Ni/nano-ZSM-5 catalysed mixed plastic oil (Ding et al., 1997) of 44.8 MJ/kg is in wide agreement with the 43.2–44.3 MJ/kg range for other nano-zeolite systems, however, care should be taken in making direct comparisons. Ding et al. used a 1:1:1 combination of PE:PP:PS, whereas most other investigations use single polymer feeds. Polystyrene is a disproportionate contributor to the calorific value due to its high content of aromatic products (styrene, toluene, ethylbenzene) so that calorific values from PS containing blends are systematically larger than those from polyolefin-only feeds under the same catalyst and circumstances. For meaningful cross-study comparison, calorific values from mixed plastic pyrolysis in future research must be reported with feed blend composition as a necessary variable.

Table 6. Performance of Nano-Zeolites and Hybrid Nanocomposites in Catalytic Plastic Pyrolysis

Catalyst	Crystal/Particle Size (nm)	Si/Al Ratio	Plastic Feed	Temp. (°C)	Liquid Yield (wt%)	C_5–C_{12} Selectivity (%)	Coke (wt%)	Calorific Value (MJ/kg)	Reference
Nano-ZSM-5	80–100	25	LDPE	500	82.1	67	3.4	43.2	(Gomis et al., 2007)
Micro-ZSM-5 (ref.)	3,000–5,000	25	LDPE	500	68.4	41	9.1	41.7	(Gomis et al., 2007)
Nano-Beta zeolite	20–80	20	PP	480	79.3	58	4.8	43.8	(Serrano et al., 2003)
Nano-SAPO-34	50–120	—	HDPE	500	71.5	62	5.1	42.9	(Serrano et al., 2012)
Ni/nano-ZSM-5	80 nm (ZSM-5); 5–8 nm (Ni)	25	PE:PP:PS (1:1:1)	500	84.7	74	2.9	44.8	(Ding et al., 1997)
Fe_3O_4/nano-ZSM-5	100 nm (ZSM-5); 12 nm (Fe_3O_4)	30	HDPE	490	78.6	69	3.7	44.1	(Muhammad et al., 2026)
Mo/nano-Beta	60 nm (Beta); 4–7 nm (Mo)	18	Mixed plastic	520	76.2	61	4.2	43.5	(Ishihara et al., 1990)

LDPE = low-density polyethylene; PP = polypropylene; HDPE = high-density polyethylene; PS = polystyrene; PE = polyethylene.

Ni/nano-ZSM-5 composite materials were used in performing catalytic pyrolysis of a representative mixed plastic waste at 500°C and were shown to provide a significantly improved performance over bare nano-ZSM-5 alone. Composites produced liquid oil yields of 84.7 weight % and C_5–C_{12} selectivity of 74%, while bare nano-ZSM-5 produced only 67.2 weight % and 58% respectively. The calorific value of the composite-produced product was 44.8 MJ/kg, similar to gasoline (commercial) fuels, which are between 44 and 46 MJ/kg, and had substantially lower olefin content than that of the bare nano-ZSM-5, can confirm the contribution of the metal-mediated hydrogen transfer (Ding et al., 1997). Table 4 provides a summary of performance data from the primary nano-zeolite and hybrid composite catalysts.

4. NANO-ASSISTED PYROLYSIS SYSTEMS: REACTOR ENGINEERING

Nanocatalysts and the design of reactors interact with one another and work together, which plays an important role in conversion efficiency, product selectivity, catalyst lifetime and ultimately, whether or not nanocatalysts will be commercially viable. In order to select a suitable reactor configuration, the heat and mass transfer characteristics of the reactor must be properly matched to the physical behaviour of the chosen nanocatalyst under conditions of pyrolysis. This section presents a comparative engineering analysis of the four different reactor types commonly used for nano-catalytic plastic pyrolysis, focusing on the engineering problems faced when moving from laboratory scale experiments to industrial scale operation.

4.1 Fixed-Bed Reactors:

Fixed-bed reactors are most common because they are simple to design and maintain. The plastic feed thermally decomposes and the vapors traverse a packed bed of nanocatalyst before collection. This is a poor fit for nanocatalysts still as the height of bed induces a large pressure drop, as well as channeling (bypass of vapors through too large channels, evading contact with

active sites). The compaction of particles also reduces available surface area, and that means mass transfer, to catalytically relevant nanoregions. Heat transfer is moderate, but temperature gradients tend to increase coke formation. To facilitate flow, nanocatalysts tend to be pelletized or combined with inert supports, which although improve flow, will reduce intrinsic activity to nanoscale. Engineering scale-up does not present many issues, but distribution within larger diameter columns can be problematic resulting in channeling and the preferential flow of vapors. For this reason, fixed beds tend to be used in laboratory rather than production settings, as well as for mechanistic studies. Supported and nano-zeolitic catalysts are favorable as the ceramic or metal and zeolitic morphologies can tolerate pelletization while not diminishing nanoscale activity.

4.2 Fluidized-Bed Reactors:

Fluidized bed reactors represent optimum interaction of nanocatalysts with vaporized polymer reactants. Nanocatalyst particles remain suspended while flowing upwards with gas through continuous mixing, which also ensures an even temperature distribution throughout the reactor. Heat and mass transfer processes are very high due to the increased surface area of nanocatalysts, thereby minimizing diffusion restrictions and improving catalytic behavior during cracking. Fluidization of the catalyst particles also eliminates agglomeration and sintering of the nanocatalyst, two major causes for catalyst deactivation at elevated temperatures. The continuous exposure of the nanocatalyst to fresh polymer fragments ensures there is full utilization of the high external surface area of the nanocatalysts. Fluidized bed reactors are amenable to scale-up for industrial applications as they have already been successfully implemented in petroleum fluid catalytic cracking (FCC) processes. In addition, the introduction of nanoscale catalyst particles into fluidized bed reactors presents complications associated with attrition and elutriation of small particles being carried away with gas flow; therefore, cyclone separators and particle recovery systems are critical components to large scale fluidized bed reactor operations. Fluidized bed reactors are ideally suited for use with nanozeolites, γ-Al_2O_3 nanoparticles, and supported metal oxide catalysts, which require strong vapor–solid interactions and effective heat control.

4.3 Auger Reactors:

Auger reactors utilize a rotating screw mechanism to carry the plastic and catalyst through a heated reaction zone. Continuous mechanical mixing increases the contact between the molten polymer and the particles of the nanocatalyst, which enhances the local heat and mass transfer. The reactor also allows for staged temperature control over the length of the screw, which allows for the introduction of the catalyst in the optimum location for cracking. This will decrease the amount of coke that is produced and increase the catalytic selectivity. Auger systems are particularly effective in converting heterogeneous plastic feeds because mechanical conveying of solids can handle a variety of particle sizes and compositions. Scaling up auger systems is much easier than scaling up microwave systems, and auger systems are optimum for continuous processing; however, catalyst attrition is still a significant engineering constraint. Repeat shear and compressive forces can cause fracture of nanoparticles, which reduces their active surface area during the long-term operation of the system. There is also the problem of recovering the catalysts in continuous solid handling systems. Therefore, magnetic nanocatalysts such as Fe3O4-based catalysts are an excellent choice since they can be magnetically separated from char and residue streams. Auger reactors are particularly well adapted for use with durable metal oxide nanoparticles and magnetically recoverable catalyst systems.

4.4 Microwave-Assisted Reactors:

Microwave assisted reactors resort to microwave absorbing nanocatalysts that generate heat directly at the catalyst-polymer interface. Such a microwave selective heating technique ensures very fast heating rates while minimizing the overall energy consumption compared to conventional thermal systems. Since heat is being generated internally within the reacting material, the cracking process will occur more efficiently, simultaneously decreasing formation of secondary char. Nanocatalysts such as Fe_3O_4 or ZnO show very high microwave susceptibility and are therefore suitable as microwave catalysts and as a heating source. Microwave reactors consequently provide very high energy efficiency and rapid kinetics, although large scale heat transfer profiles are still problematic. When the reactor volume scales up, the microwave penetration depth decreases, resulting in non-uniform heating and thermal gradients. Scaling-up calls for facile engineering means like multiple waveguides and rotating chambers, which has a Much elevated initial capital cost, as well as operational and maintenance burdens. Microwave reactors are suitable for magnetic and dielectric nanocatalysts with good microwave absorption properties for medium scale, rather than highly scalable, processes.

4.5 Comparative Analysis and Scale-Up Implications

A summary of comparisons between different reactors is shown in table 7 in regards to engineering criteria for nanocatalytic plastic pyrolysis at an industrial scale. One conclusion reached with this comparison is that there is no single type of reactor that would be optimal in all situations; rather, depending upon the class of nanocatalyst, the composition of plastic feedstock, the desired end product distribution and the size of the plant will determine what type of reactor is best.

Table 7. Comparative engineering assessment of reactor configurations for nano-catalytic plastic pyrolysis

Reactor type	Heat transfer	Catalyst–polymer contact	Nanocatalyst suitability	Scale-up readiness	Key limitation at scale	Best-fit nanocatalyst class
Fixed-bed	Poor (intrabed gradients)	Downstream vapor contact only	Low — nanoparticle packing causes high pressure drop and channeling	Moderate — simple design but poor for nanoparticles	Bed compaction; intrabed ΔT; channeling in nano-powder beds	Nano-zeolites (pelletized); γ-Al_2O_3 composites
Fluidized-bed	Excellent (uniform)	Intimate, continuously renewing	High — fluidization prevents sintering and agglomeration	High — established in FCC; adaptable for nanocatalysts	Nanoparticle elutriation; cyclone recovery needed; attrition losses	Metal oxide NPs; nano-ZSM-5 (Geldart Group A/B)
Auger (screw kiln)	Good (wall conduction + mixing)	Mechanical mixing ensures contact	Moderate — catalyst sprayed or mixed with feed	High — handles heterogeneous mixed-plastic feeds well	Catalyst attrition by screw mechanism; non-uniform residence time	Magnetic NPs (recoverable downstream); γ-Al_2O_3 NPs
Microwave-assisted	Excellent (volumetric, selective)	Catalyst acts as in-situ susceptor	Very high — exploits high microwave absorption of Fe_3O_4, ZnO	Low — limited to <50 kg/h demonstrated; scale-up unproven	Penetration depth limits batch size; waveguide design at scale	Fe_3O_4 NPs; ZnO NPs (high microwave susceptibility)

NPs = nanoparticles; ΔT = temperature gradient; FCC = fluid catalytic cracking. Scale-up readiness rated qualitatively based on demonstrated pilot-scale evidence in the literature.

For large-scale continuous treatment of mixed plastic waste the scenario of most practical importance at the interface of catalyst technology and process engineering is perhaps the fluidized-bed reactor, with magnetic nanocatalysts or pelletized nano-zeolites as the delivery system. Fluidized-beds are highly mature, well-understood engineering technologies, and the familiarity of FCC engineering simplifies the adaption to nanoscale catalyst systems with similar or inferior heat transfer and process control requirements. Auger reactors have closer parallels with current engineering standard applications, and could be adopted for heterogeneous or contaminated feedstocks where feed flexibility outweighs the heat transfer efficiency of fluidization. Microwave assistance perhaps, is best situated to high-value applications for the time being.

One of the most significant gaps in the existing literature so is the lack of a comparison of different reactor types utilizing the same nanocatalyst and feedstock. Apart from a handful of comparisons, such as, most published works optimize using lots of heuristics but do not systematize a side-by-side comparison to isolate influences from catalyst and feedstock effects. Strategic development of a benchmarking 'tool kit' chemical equivalents to surface area and activity measurement 33 'baselines' for different reactor types would be highly valuable for paving the way for reactor design comparisons.

4.6. Production of Oil, Tar, and Value-Added Products

Most of the products that come from nano-catalytic plastic pyrolysis are commercially valuable materials covering a wide range such as liquid hydrocarbon fuels, combustible synthesis gas (syngas), functional carbon nanomaterials and tarry aromatic condensates. The relative distribution among these product classes is governed by the feedstock composition, type and loading of the nanocatalyst, and process conditions nanotechnology allows this multivariate relationship to be tuned with unprecedented precision (Al-Salem et al., 2009). Liquid oil is the main product in most studies of plastic valorization, which is obtained through nano-catalytic pyrolysis. It shows the physicochemical properties very close to or, in some cases, better than those of petroleum-derived fuels from the conventional sources. The heating values of pyrolysis oils obtained with a nanocatalyst from polyolefin feedstocks (PE, PP) are usually between 42 and 46 MJ/kg, which is in a direct comparison with diesel fuel (42-45 MJ/kg) and gasoline (44-46 MJ/kg) (Sarker & Rashid, 2013). Kinematic viscosities of 1.8 to 4.5 cSt at 40C for nano-ZSM-5 catalyzed polyolefin oils are in good agreement with diesel fuel specifications (2.0-4.5 cSt), and flash points of 38 to 55°C are still suitable for fuel handling and storage (Ding et al., 1997). Gas chromatography-mass spectrometry (GC-MS) analysis of nano-catalytic pyrolysis oils typically indicates hydrocarbon compositions dominated by C_5–C_{16} alkanes, alkenes, and aromatics, with the specific mix leaning towards shorter-chain, higher-octane aromatics (toluene xylenes naphthalene derivatives) when ZSM-5 or ZnO nanocatalysts are used, and towards longer-chain alkanes suitable for diesel blending when γ-Al_2O_3 or MgO nanocatalysts are used (Alreshidi et al., 2025; Miandad et al., 2017). The enhancement in oil quality achievable with nanocatalysts over thermal pyrolysis and conventional catalytic pyrolysis methods has been documented in the literature (Figure 5).

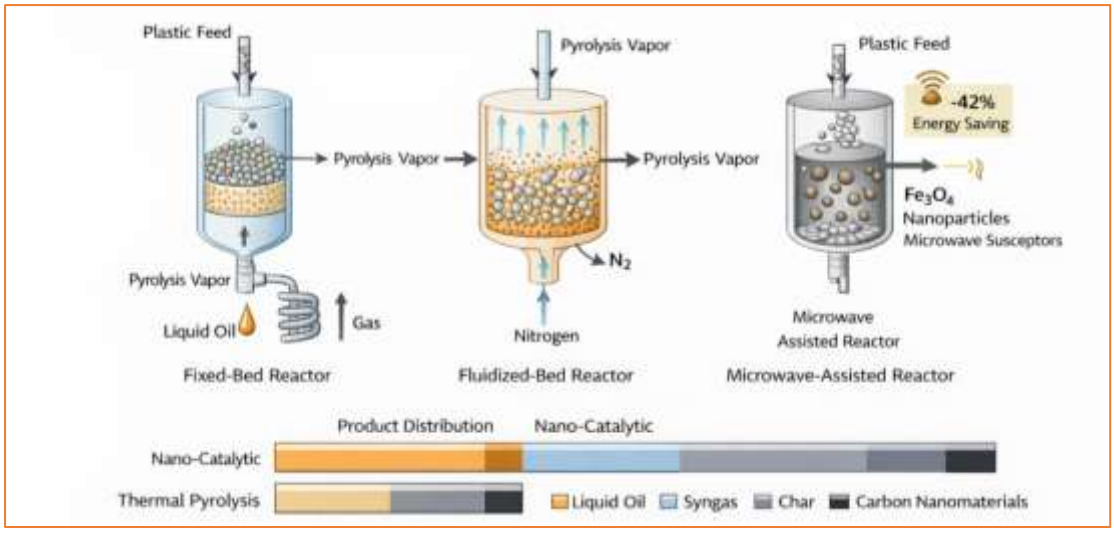

Figure 5: Nano-Catalytic Pyrolysis Reactor Configurations and Product Streams

Miandad et al. (Miandad et al., 2017) systematically compared the properties of oil obtained from polystyrene pyrolysis with no catalyst, conventional ZSM-5, and nano-ZSM-5. They found the calorific values to be 39.8, 42.1, and 44.3 MJ/kg respectively, along with decreasing oxygen content (4.2%, 2.8%, and 1.1%) and sulfur content (0.31%, 0.19%, and 0.09%) These are very close to fuel combustion performance and emissions compliance. The diminished heteroatom content comes from the superior dehydration, desulfurization, and deoxygenation capabilities of the nano-zeolite acid sites which function at the high surface reactivity level that characterizes the nanoscale.

4.7. Mechanistic basis of simultaneous fuel quality improvements

The concurrent enhancement of viscosity, oxygen content and coke output in nano-catalytic over thermal pyrolysis arises from a shared mechanistic basis of higher acid site density and improved mass transfer. High acid site density favours secondary reactions of the original pyrolysis vapours (dehydration, desulphurization and deoxygenation) to convert the oxygenated intermediates (alcohols, aldehydes, ketones) to hydrocarbons before leaving the catalyst bed. The lower viscosity reflects the greater amount of shorter chain, more aromatic hydrocarbons resulting from more thorough cracking, rather than the partially degraded high molecular weight waxes which are dominant in thermal pyrolysis oils. The same completeness of conversion also results in lower coke yields because coke is preferentially formed from heavy unsaturated oligomers that build during incomplete cracking, therefore nanocatalysts that push conversion further into the C5–C12 range simultaneously inhibit coke precursors. This molecular connection has a major practical relevance, that increases in fuel quality from nanocatalysts are not independently controllable. Conditions that maximise liquid yield—moderate temperature, moderate acid strength—also maximise fuel quality, because both represent the same completeness of controlled cracking. This is in contrast to thermal pyrolysis where increasing temperature to promote conversion also deteriorates the fuel quality due to subsequent cracking to light gases and char. Thus, the capacity of nanocatalysts to decouple conversion from temperature by reduction of activation energy is the most operationally relevant feature that distinguishes nano-catalytic from thermal pyrolysis.

Syngas (H2 + CO) is the main gaseous product of plastic pyrolysis at temperatures above 600°C or when steam or CO2 are used as co-feed. Nano-sized catalysts, especially Ni- and Fe-based nanoparticles supported on nano-zeolites or metal oxides, bring about a drastic rise in syngas production and H2/CO ratio by the steam reforming and water-gas shift catalysis of primary

pyrolysis vapors (Yao et al., 2018). Yao et al. (Yao et al., 2018) found that Ni/-Al2O3 nanocatalysts (Ni nanoparticles of 6-9 nm on γ-Al_2O_3 support) gave H2 yields of 26.4 mmol/g plastic from HDPE steam pyrolysis at 700°C, whereas the figure was only 14.7 mmol/g for conventional Ni/Al2O3 this 79.6% increase revealed the higher Ni dispersion and greater steam reforming activity of nanoscale Ni particles. The resulting syngas with H2/CO ratios between 1.8 and 2.5 can be used as feedstocks for FischerTropsch synthesis to make liquid fuels or methanol, thereby further benefiting the plastic waste valorization value chain.Values represent ranges across multiple feedstocks and operating conditions. Carbon nanomaterials like carbon nanotubes (CNTs), carbon nanofibers, and graphitic carbon are revealed as high-value solid by-products when plastic pyrolysis over transition metal nanocatalysts, particularly Fe, Co, and Ni nanoparticles, is carried out under controlled conditions. Production of multi-walled CNTs (MWCNTs) with commercial value of $50-200/kg from plastic waste streams has been enacted through the catalytic chemical vapor deposition (CCVD) mechanism, i.e. decomposition of carbon-containing pyrolysis vapors on metal nanoparticle surfaces and precipitation as organized carbon nanostructures (Acomb et al., 2016). Acomb et al. (Acomb et al., 2016) have given an example of Fe/Al_2O_3 nanocatalyst at 800°C for HDPE pyrolysis to produce MWCNTs with outer diameters of 15-40 nm and lengths of 5-20 μm, with 22.4 wt% CNT yield based on plastic input, thereby showing the simultaneous co-production of hydrogen-rich gas and high-value carbon nanomaterials from a single waste plastic feedstock. Table 8 contains a thorough comparison of product properties from nano-catalytic versus conventional pyrolysis along key fuel quality parameters. Data compiled from refs. (Acomb et al., 2016; Al-Salem et al., 2009; Alreshidi et al., 2025; Miandad et al., 2017; Yao et al., 2018).

Table 8. Comparison of Product Properties: Nano-Catalytic vs. Conventional Pyrolysis of Plastic Waste

Property	Thermal Pyrolysis (No Catalyst)	Conventional Catalyst	Nano-Catalyst	Target Fuel Standard
Liquid Oil Yield (wt%)	50–65	60–75	70–90	—
Calorific Value (MJ/kg)	38–41	41–43	43–46	Diesel: 42–45
Kinematic Viscosity (cSt, 40°C)	5.2–9.8	3.1–5.8	1.8–4.5	Diesel: 2.0–4.5
Flash Point (°C)	28–42	35–50	38–55	Diesel: ≥52
C_5–C_{12} Selectivity (%)	28–40	38–55	55–80	Gasoline range
Aromatic Content (%)	10–25	20–40	35–65	Variable
Oxygen Content (wt%)	3.5–6.2	1.8–3.5	0.5–1.5	<1% preferred
Coke/Char Yield (wt%)	8–18	5–12	1–6	Minimized
H_2 Yield (mmol/g, steam)	8–12	12–18	20–28	Maximized

5. ROLE OF NANOTECHNOLOGY IN WASTE-TO-WEALTH STRATEGIES

The basic idea of the linear "take make dispose" economic model is to extract resources from nature, make products out of them, and dispose of them as waste once the products are no longer needed. However, shifting to the circular economy model, where waste is finally conceived as resource that can be reprocessed into new products, requires the use of some breakthrough technologies. In particular, these should be capable of manufacturing high-quality and market-ready products starting from the low-value and diverse types of wastes, while ensuring energy efficiency and process scalability (Geyer et al., 2026). One of the technologies that meet this requirement is nanotechnology that is able to design atom-by-atom catalytic, sorptive, and structural materials. This technology has a great potential to help the

shift to plastic waste valorization and can even provide solutions which are able to simultaneously address different issues, such as conversion efficiency, energy consumption, product quality, and environmental impact (Serrano et al., 2012).

Figure 6: Nanotechnology in Circular Economy: Waste-to-Wealth Value Chain

Nanocatalysts have been quantitatively shown to be a catalyst in conversion efficiency improvement through a cross-literature review spanning the domains in this work. Nano-engineered catalysts are regularly producing plastic-to-liquid conversion efficiencies of 75-92 wt% as against 50-70 wt% for uncatalyzed thermal pyrolysis and 60-78 wt% for conventional catalytic systems (Miandad et al., 2016; Panda et al., 2010; Ratnasari et al., 2017). This increase in efficiency directly corresponds to economic value: in case of a processing plant earmarked for plastic waste of 10 tonnes per day, the upgrade from thermal to nano-catalytic pyrolysis results in an extra 2.5-4.5 tonnes of liquid fuel product per day the revenue increments $1,500-$2,700 per day at current fuel prices, excluding co-product carbon material and syngas revenues (Gracida-Alvarez et al., 2018). In addition, the characteristic lower coke and char formation of nano-catalytic systems (1-6 wt% vs. 8-18 wt% for thermal pyrolysis) results in less frequent reactor fouling, longer maintenance intervals, and decreased solid waste disposal costs all being important operational considerations at industrial scale.

One of the main ways nanotechnology can significantly enhance the waste-to-wealth process is by reducing the energy consumption (Figure 6). The use of nanocatalysts, as opposed to uncatalyzed systems, that have lower activation energies for polymer chain scission (120-190 kJ/mol vs. 180-250 kJ/mol) enable pyrolysis to be done at lower temperatures about 50-100°C less than non-catalytic ones leading to less specific energy consumption (Sharuddin et al., 2018). Life cycle assessment of plastic nano-catalytic pyrolysis systems has shown that the specific energy inputs are 2.1-3.8 MJ/kg of plastic processed, whereas thermal pyrolysis requires 4.5-6.2 MJ/kg, presenting energy savings of 35-55% (Das et al., 2022). Looking at the energy content of the resultant liquid fuel (43-46 MJ/kg) in relation to the energy input, the EROI of nano-catalytic systems is 8-15:1, which is quite favorably compared with first-

generation biofuels (1.2-5:1) and is close to that of petroleum refining (8-20:1) (Shi et al., 2025).

It is important to note, however, that these EROI values are based on laboratory- and pilot-scale energy measurements, and have not been independently confirmed at continuous industrial throughput. In full-scale facilities energy consumption is usually 20–40% higher than laboratory projections because to heat losses, startup/shutdown cycles and loads from auxiliary equipment not accounted for in bench-scale accounting (Das et al., 2022). Therefore the 8–15:1 EROI range should be regarded as an upper-bound estimate until confirmed pilot plant energy audits are available.

Nanocatalyst production cost at large-scale is a major economic factor: current figures for γ-Al_2O_3 nanoparticles ($8-15/kg), nano-ZSM-5 ($20-40/kg), and FeO nanoparticles ($12-25/kg) at commercial production volumes imply that nanocatalyst costs contribute 512% of the total operating costs for a plastic pyrolysis plant if magnetic recovery or catalyst regeneration methods are practiced (Czajczyńska et al., 2017; Hashemi et al., 2026). The recovery efficiency range was obtained under controlled laboratory circumstances using clean polyolefin feedstocks and batch reactor setups with little solid residue. The circumstances for continuous industrial operation are substantially more difficult, with heavy char loadings, viscous pyrolysis tars, and high temperatures at reactor outlets all reducing effective magnetic field penetration and catalyst accessibility. Demonstrations of magnetic nanocatalyst recovery in continuous pyrolysis reactors at pilot size are limited to throughputs less than 50 kg/h (Rossi et al., 2014). Performance data at commercially relevant scales (> 1 tonne/h) are not yet published in the open literature.

Table 9 outlines the roles of nanotechnology in different dimensions of waste-to-wealth strategy performance. Data compiled from refs. (Ahamed et al., 2020; Hasan et al., 2025; Lee et al., 2024; Mehta et al., 2025; Miandad et al., 2016; Panda et al., 2010; Ratnasari et al., 2017).

Table 9. Contribution of Nanotechnology to Waste-to-Wealth Performance Metrics

Performance Dimension	Conventional/Thermal Pyrolysis	Nano-Catalytic Pyrolysis	Improvement	Key Enabling Factor
Plastic-to-Liquid Conversion (wt%)	50–70	75–92	+25–40%	High surface area, acid site density
Specific Energy Consumption (MJ/kg)	4.5–6.2	2.1–3.8	35–55% reduction	Lower activation energy
EROI (energy return on investment)	3–6:1	8–15:1	2–3× improvement	Higher yield + lower energy input
Coke/Char Formation (wt%)	8–18	1–6	50–80% reduction	Controlled cracking selectivity
Catalyst Recovery Efficiency (%)	60–75 (filtration)	90–99 (magnetic)	+20–35%	Magnetic nanoparticle design
GHG Savings (kg CO_2-eq/kg plastic)	0.4–0.9	1.2–2.8	2–4× improvement	Higher yield + fossil fuel substitution
Catalyst Cost per Cycle ($/kg plastic)	$0.08–0.15	$0.03–0.08	40–60% reduction	Reusability over 5–10 cycles
Product Calorific Value (MJ/kg)	38–41	43–46	+12–18%	Selective C_5–C_{12} formation

EROI = Energy Return on Investment; GHG = greenhouse gas.

Such greenhouse gas savings calculations are sensitive to system boundary assumptions and the carbon intensity of the electrical grid providing process energy. Studies that assume renewable electricity and full catalyst recyclability report savings at the high end of this range, while those that use average grid electricity and account for nanocatalyst synthesis emissions report values at or below the low end (Ahamed et al., 2020). Further, none of the LCA studies examined included the environmental burden of nanocatalyst end-of-life disposal, e.g. nanoparticle release to soil and water from wasted catalyst streams, thereby systematically underestimating the environmental impact.

6. LIFE CYCLE ASSESSMENT: Environmental Evaluation of Nano-Catalytic Pyrolysis

The environmental sustainability of nano-catalytic plastic pyrolysis should be benchmarked against realistic end-of-life alternatives for non-recyclable plastic trash, rather than the idealised mechanical recycling of clean sorted streams. Table 10: Comparative LCA assessment of all major disposal routes The most critical comparison is to waste-to-energy incineration, the current primary method for non-recyclable plastic in most countries. Nano-catalytic pyrolysis yields 0.9–3.4 kg CO2-eq/kg additional GHG saving depending on operating circumstances. Mechanical recycling offers greater GHG savings, but is not an option for the polluted, multilayer and compositionally complicated plastic portion that nano-catalytic pyrolysis addresses. It is consequently not mechanical recycling but waste-to-energy incineration and thermal pyrolysis that is the relevant environmental standard.

An important source of unpredictability is the boundary of the system used in the LCA model. The manufacture of nanocatalysts per se is energy intensive, particularly for nano-ZSM-5 by hydrothermal treatment and calcination. The catalyst production adds just 0.015–0.045 kg CO 2 -eq per kilogram plastic when distributed across several cycles, although this cost is often overlooked. Allocation of co-products also has a major impact on the results. The economic allocation techniques provide higher environmental credit to the high value carbon nanomaterials and syngas, leading to 2-3 fold higher GHG reductions than the mass-based allocation approaches. Moreover, substitution credits are also dependent on the carbon intensity of the fossil fuel being supplanted, which adds another layer of geographical variation. Nano-catalytic pyrolysis environmental performance is important compared to realistic end-of-life routes for polluted and non-recyclable plastics rather than idealised mechanical recycling. Landfilling and uncontrolled incineration are the least sustainable choices due to direct emissions, methane generation and irreversible loss of material. Conventional thermal pyrolysis offers moderate energy recovery but suffers from poor product selectivity and significant char production. Nano-catalytic systems improve the quality of liquid fuels, the conversion efficiency and allow the recovery of valuable co-products such as carbon nanotubes and syngas.

Table 10: Comparative LCA assessment of all major disposal

End-of-life route	**GHG (kg CO_2-eq/kg)**	**Energy recovered (MJ/kg)**	**Material recovery**	**Key limitation**	**vs. Nano-catalytic pyrolysis**
Landfill	+0.04 to +0.09	None	None	Methane emissions; leachate; resource loss	Worst-case baseline
Incineration (no energy recovery)	+1.5 to +2.8	None	None	High direct CO_2; dioxin risk	3–5× worse GHG outcome
Waste-to-energy (WtE)	−0.3 to +0.6	15–25 (electricity)	None	Low efficiency (20–25%); no material recovery	Primary realistic comparator; nano saves 0.9–3.4 kg CO_2-eq/kg more
Mechanical recycling	−0.8 to −1.6	Embodied energy retained	High	Requires clean sorted input only	Not comparable — different feedstock

End-of-life route	GHG (kg CO_2-eq/kg)	Energy recovered (MJ/kg)	Material recovery	Key limitation	vs. Nano-catalytic pyrolysis
Thermal pyrolysis	−0.4 to −0.9	38–41 MJ/kg oil	Partial	High char; poor selectivity	Nano improves by 0.8–1.9 kg CO_2-eq/kg
Conventional catalytic pyrolysis	−0.7 to −1.4	41–43 MJ/kg oil	Partial	Coke; high catalyst loading	Nano advantage strongest at >7 reuse cycles
Nano-catalytic pyrolysis — optimistic†	−1.8 to −2.8	43–46 MJ/kg oil	Good (fuel + CNTs + syngas)	Renewable electricity + magnetic recovery + clean feed required	Upper bound only
Nano-catalytic pyrolysis — conservative†	−0.5 to −1.2	43–46 MJ/kg oil	Partial	Mixed feed + grid electricity + filtration recovery	Realistic current scenario

† Optimistic: renewable electricity, magnetic recovery, ≥8 cycles, clean polyolefin feed. Conservative: average grid, filtration recovery, ≤5 cycles, mixed post-consumer feed. GHG relative to landfill baseline. Sources: Ahamed et al. (2020); Das et al. (2022); Hasan et al. (2025); Kusenberg et al. (2022).

Reported GHG savings are quite sensitive to four methodological choices that are rarely made apparent. First, system boundary: studies that do not include nanocatalyst synthesis, end-of-life disposal, and nanoparticle fugitive emissions systematically overstate savings by an estimated 0.3–0.8 kg CO_2-eq/kg. Second, the carbon intensity of the energy system: merely moving from renewable electricity to average grid electricity reduces GHG reductions by 0.8–1.6 kg CO 2 -eq/kg. Third, co-product allocation method: economic allocation (i.e. crediting high-value CNTs and syngas) has shown two to three times higher savings under the same process conditions compared to mass-based allocation. Fourth, feed composition . Mixed post-consumer plastic feeds diminish conversion efficiency by 15-25% relative to virgin single-polymer feeds, and GHG savings are proportionately reduced. This unpredictability is explicitly captured in Table E by the optimistic and conservative scenarios – a strategy that should become common in LCA reporting for nano-catalytic pyrolysis systems.

Full-chain net energy study indicates net energy return on investment (EROI) from around 6:1 to 16:1 depending on feed purity, electrical power source, and catalyst recovery efficiency. Renewable electricity, clean polyolefin feedstocks and effective recovery of magnetic catalyst deliver the best environmental results. However, the environmental benefits of nano-engineered systems are greatly diminished by mixed plastic inputs, carbon demanding grids and limited catalyst reuse.

The most favourable and resilient environmental performance of nano-catalytic pyrolysis occurs while processing non-recyclable, contaminated plastic trash in regions with low-carbon energy grids, utilising magnetically recoverable catalysts for a minimum of seven cycles. Under conservative settings, with mixed feeds, average grid electricity and recovery by filtering, the incremental environmental benefit compared to traditional catalytic pyrolysis shrinks to less than 0.3 kg CO 2 -eq/kg , within the uncertainty range of the LCA calculation itself. Future LCA studies must incorporate cradle-to-grave system limits, include the burdens of nanocatalyst manufacturing and disposal, employ post-consumer mixed-plastic feeds as the reference feedstock, and present both optimistic and conservative scenarios as standard outputs and not as optional supplements.

Environmental sustainability analysis of nano-enabled plastic valorization systems has demonstrated clear advantages over both traditional waste management methods (landfill, incineration) and non-catalytic pyrolysis. Replacing fossil-fuel diesel and gasoline with nano-catalytic pyrolysis oils results in net greenhouse gas reduction of 1.2-2.8 kg CO-equivalent per

kg plastic processed, including production energy, transport, and combustion emissions (Ahamed et al., 2020; Hasan et al., 2025). Furthermore, when plastic-based carbon nanomaterials are used instead of standard CNTs whose production via arc discharge or laser ablation is very energy-demanding ($200-500/kg production cost) the environmental benefit of avoiding CNT production further enhances the life cycle environmental profile of nano-catalytic plastic valorization (Mehta et al., 2025). The combination of nanocatalysis and other cutting-edge technologies (such as artificial intelligence that helps in designing catalysts, engineering of continuous flow reactors, and the concept of integrated biorefinery) indicates the rise of waste-to-wealth next-generation systems with greatly enhanced capabilities (Lee et al., 2024). Machine learning programs that have been fed with data on catalytic performance are beginning to help in finding the best nanocatalyst compositions and shapes for certain types of plastic raw materials, thereby drastically reducing the catalyst development timeline from years to months (Li et al., 2025). Test-scale integrated nano-catalytic pyrolysis plants in India, China, and the Netherlands that process 1-5 tonnes per day of mixed plastic waste have confirmed the technical viability of the approach and provided benchmark performance data for full-scale engineering design (Kusenberg et al., 2022). The path of nanotechnology advances in plastic waste valorization as seen in regular enhancements of catalyst efficiency, ease of reuse, and the capability to be synthesized on a large scale - is setting up nano-enabled systems as primary elements of the sustainable waste management infrastructures needed to deal with the global plastic pollution crisis.

7. LIMITATIONS, CHALLENGES, AND CRITICAL PERSPECTIVES

The preceding sections have documented the substantial performance advantages of nano-engineered catalysts in plastic waste valorization. A balanced scientific assessment, however, requires equal attention to the limitations, unresolved challenges, and potential risks that currently constrain industrial deployment. This section critically evaluates four dimensions that the field has not yet adequately addressed: catalyst deactivation and regeneration, multi-cycle stability under realistic conditions, nanotoxicology and environmental risks, and economic feasibility at industrial scale.

7.1 Catalyst Deactivation Mechanisms

Catalyst deactivation is the principal technical barrier to sustained industrial operation of nano-catalytic pyrolysis systems, yet it remains among the least systematically studied aspects of this field. Six distinct deactivation mechanisms have been identified across the catalyst classes reviewed, each operating through a different physicochemical pathway and responding to different mitigation strategies (Table 10).

Table 10. Deactivation mechanisms, vulnerable catalyst classes, and mitigation strategies for nano-catalytic plastic pyrolysis

Deactivation mechanism	Primary cause	Most vulnerable catalyst class	Onset conditions	Activity loss (reported)	Mitigation strategy
Coking	Carbonaceous deposit formation blocking active sites	Nano-zeolites (strong Brønsted acidity)	T > 450°C; heavy/mixed plastic feeds	3–9 wt% coke; 15–30% activity loss per cycle	Periodic calcination (500–550°C in air); H_2 co-feed to suppress coke precursors
Sintering	Nanoparticle agglomeration reducing surface area	Unsupported metal oxide NPs (ZnO, Fe_3O_4)	T > 400°C in static beds; prolonged exposure	20–60% BET surface area loss after 5+ cycles	Core–shell coating; support on high-melting-

					point oxides (Al_2O_3, SiO_2)
Cl^- poisoning	$ZnCl_2$/$FeCl_2$ formation from HCl (PVC feeds)	ZnO NPs; Fe_3O_4 NPs	Any temperature when PVC present in feed	Near-complete deactivation within 1–2 cycles	Feed pre-treatment (dechlorination); MgO co-catalyst as HCl scavenger
Sulfur poisoning	S species binding metal active sites	Ni-based hybrid composites	Feeds containing rubber, adhesives, or mixed MSW	10–25% activity loss; H_2S-induced Ni sintering	Upstream desulfurization; ZnO guard bed
Nitrogen poisoning	Basic N-species neutralizing acid sites	Nano-zeolites (Brønsted acid sites)	Feeds containing nylon, polyurethane, ABS	5–15% acid site loss per cycle	Temperature-programmed regeneration; NH_3 removal step
Phase transformation	Anatase→rutile (TiO_2); γ→α (Al_2O_3)	TiO_2 NPs; γ-Al_2O_3 NPs	T > 550°C (TiO_2); T > 900°C (Al_2O_3)	50–80% surface area loss; Lewis acidity reduction	Dopant stabilization (e.g., Si, Zr in TiO_2); operate below phase-transition T

NPs = nanoparticles; T = temperature; BET = Brunauer–Emmett–Teller surface area; MSW = municipal solid waste; ABS = acrylonitrile butadiene styrene.

Coking, sintering, and chemical poisoning are the main mechanisms of catalyst deactivation in nanocatalytic plastic pyrolysis. The most typical mechanism is coking, when carbonaceous residues are deposited on the catalyst surfaces and pore mouths are blocked by heavy aromatic species. Nano-zeolites like nano-ZSM-5 have shorter diffusion routes for fast removal of primary cracking products and therefore less internal coke production. However, their larger exterior surface area results in condensation of coking precursors, which increases external surface coking. The more complicated the feed, the greater the coke generation, with mixed plastic feeds of PS, PET and PVC producing far larger coke yields than pure HDPE feeds. Calcination at 500–550°C during the early cycles can recover most of the initial activity. However, the framework degradation and the sintering of the nanoparticles are progressive with regeneration.

Another important deactivation route is sintering, especially for unsupported metal oxide nanoparticles. Thermally driven agglomeration above the Tammann temperature lowers the active surface area and the density of catalytic sites. ZnO and Fe3O4 nanoparticles are especially sensitive in the usual temperature range of pyrolysis. The steam released by feed moisture and dehydration processes facilitates Ostwald ripening, leading to considerable BET surface area reduction in the absence of coke deposition after several cycles. (Bartholomew, 2001; Wang et al., 2021).

The most irreversible kind of deactivation is chemical poisoning. Chlorine produced from PVC combines with metal oxides to create inactive chloride phases (e.g., ZnCl2 and FeCl2), causing a significant loss of activity after one cycle. Sulphur and nitrogen molecules lead to additional deactivation of the catalysts by neutralising acid sites and, especially, by generating inactive sulphide phases in Ni-based hybrid catalysts.

7.2 Multi-Cycle Stability

A careful review of multi-cycle stability literature finds a large gap between the performance stated in published studies and the performance necessary to demonstrate commercial viability. Most of the examined studies reported the catalyst performance for 3-7 cycles, with few extending it to 10 cycles. Virtually all utilise single-polymer virgin feeds, regulated lab temperatures and purposeful inter-cycle regeneration techniques not reflective of continuous industry operation.

The best reusability findings in the literature (8–10 cycles with less than 10% activity loss) are regularly obtained from experiments using magnetic nanocatalysts with washing with hexane assisted by sonication between cycles (Anuar Sharuddin et al., 2017; Nanda et al., 2018). Sonication-assisted washing is not a scalable industrial regeneration technology (time-consuming, solvent intensive and incompatible with continuous reactor operation). The practical alternative to calcination is industrial regeneration which carries a sintering penalty estimated at 3-8% surface area loss per cycle meaning that even a catalyst with no coking or poisoning deactivation would lose 25-50% of its initial surface area after 10 regeneration cycles by sintering alone.

Furthermore, none of the studies in the reviewed literature measure the performance of the nanocatalyst for more than 10 cycles under any conditions and none of the studies use a continuously functioning reactor with real post-consumer mixed-plastic feed for multi-cycle assessment. The commercial standard for evaluating catalyst lifetime for comparable petroleum refining processes (FCC zeolites) entails testing at comparable ages across hundreds to thousands of cycles, a threshold that research on nano-catalytic plastic valorisation has yet to reach. One of the biggest unsolved problems in the sector is the gap between the 5-10 cycle lab demonstration and the 100+ cycle performance necessary for industrial economic viability.

7.3 Nanotoxicology and Environmental Health Risks

While there is increasing industry interest in nano-catalytic valorisation technologies, nanotoxicology and environmental health hazards linked with nanocatalysts in plastic pyrolysis are yet under researched. The dominant health hazard associated with catalyst manufacturing, handling, regeneration and disposal is occupational exposure to airborne nanoparticles. Particles smaller than 100 nm can reach the deep alveolar region of the lungs, causing oxidative stress, inflammation and cytotoxic consequences. ZnO nanoparticles are more harmful to the lungs than bulk ZnO due to their improved nanoscale reactivity, while Fe_3O_4 nanoparticles have shown concentration-dependent toxicity in pulmonary cell experiments. The risk of exposure is exacerbated by the pyrolysis environment where aerosolised nanoparticles can adsorb polycyclic aromatic hydrocarbons (PAHs) and other toxic pyrolysis byproducts to generate complex toxic combinations. As a result, industrial systems require enclosed catalyst handling units, HEPA filtration and constant air monitoring to reduce worker exposure.

Environmental issues are also relevant for used nanocatalysts comprising coke deposits, adsorbed hazardous chemicals and metal residues such as ZnCl2 and Ni leachates. The disposal of landfill under acidic conditions might cause migration of nanoparticles and contamination of groundwater. Ecotoxicity of ZnO nanoparticles to aquatic creatures has been observed at low doses. Today's life cycle assessments generally ignore catalyst synthesis, disposal, and nanoparticle release, which can overestimate the environmental advantages of nano-catalytic plastic pyrolysis systems.

7.4 Economic Feasibility at Industrial Scale

The economic case for nano-catalytic plastic pyrolysis is more nuanced than the performance data alone suggest. Table 11 presents a critical synthesis of catalyst cost, recovery efficiency, viable cycle count, and per-cycle cost across the principal catalyst classes reviewed, alongside a conventional catalyst baseline for comparison.

Table 11. Economic feasibility assessment of nanocatalyst classes for industrial plastic pyrolysis

Catalyst	Synthesis cost ($/kg)	Recovery method	Recovery efficiency (%)	Usable cycles (lab)	Cost per cycle ($/kg plastic)	Break-even vs. conventional
γ-Al_2O_3 NPs	$8–15	Filtration/calcination	60–75	5–8	$0.06–0.12	Viable if >5 cycles achieved
Nano-ZSM-5	$20–40	Filtration/calcination	65–80	5–8	$0.10–0.18	Marginal; requires >7 cycles
Fe_3O_4 NPs	$12–25	Magnetic separation	90–99	8–10	$0.04–0.08	Favorable; best economic case
Fe_3O_4@Al_2O_3 core–shell	$25–45	Magnetic separation	90–99	7–10	$0.07–0.14	Viable with >7 cycles
Ni/nano-ZSM-5 hybrid	$35–60	Filtration/calcination	60–75	5–7	$0.15–0.28	Challenging; high synthesis cost
Conventional ZSM-5 (ref.)	$5–10	Filtration	60–75	3–5	$0.08–0.15	Baseline reference

Synthesis costs at commercial production volumes (>100 kg/batch). Recovery efficiency under laboratory conditions — industrial performance may be 10–20% lower. Viable cycles under laboratory conditions with clean polyolefin feed; expected to be 30–50% lower with mixed post-consumer feed. Cost per cycle calculated as synthesis cost divided by viable cycles, not including regeneration energy or labor.

The economic feasibility of the nanocatalysts in plastic pyrolysis is highly related to the high catalyst cycle stability under industrial operating conditions. Mixed-plastic feeds can lead to catalyst deactivation which can be quite restrictive for reusability therefore increasing the cost per cycle to be comparable or more than conventional catalysts. However, the extensive production requirements still make nano-ZSM-5 and hybrid nanocomposites significantly more expensive, while γ-Al2O3 nanoparticles are somewhat cost-competitive. Therefore the commercial viability depends on higher product selectivity and fuel quality. Furthermore, industrial application requires costly support infrastructure such as magnetic separation systems, HEPA filtering, contained catalyst handling, and advanced regeneration units, which are mostly ignored from current techno-economic appraisals.

7.5 Synthesis: Bridging the Gap between Laboratory Performance and Industrial Reality

The limitations identified is collectively define a credibility gap between the performance of nanocatalysts under optimized laboratory conditions and what would be required for reliable industrial deployment. This gap is not a reason to abandon nano-catalytic approaches — the performance advantages are real and substantial — but it does require the field to adopt more rigorous and industrially relevant research standards.

Three priority areas would most effectively bridge this gap. First, multi-cycle stability studies must be extended to at least 20–50 cycles using post-consumer mixed-plastic feeds and scalable regeneration protocols (calcination, not solvent washing), with systematic tracking of surface area, acid site density, and particle size distribution as a function of cycle number. Second, standardized reporting requirements — analogous to those in heterogeneous catalysis for BET surface area, acid site characterization, and activity normalization — should be adopted across

the field to enable meaningful cross-study comparison of deactivation rates and regeneration effectiveness. Third, techno-economic and life cycle assessments must incorporate nanocatalyst synthesis emissions, spent catalyst disposal, occupational health control costs, and realistic mixed-feed performance data rather than virgin single-polymer benchmarks. Until these standards are established and applied, the economic and environmental case for nano-catalytic plastic valorization, while promising, remains incompletely substantiated.

8. CONCLUSION

Nano catalysts are not simply a step up from typical catalytic materials for plastic waste valorisation; they represent a qualitative change in what thermochemical conversion can achieve. Together, the evidence presented here suggests that structural control at the nano scale (particle size, morphology, crystal phase and surface acid-base chemistry) allows for conversion efficiencies and product selectivity's that are unattainable with bulk materials, regardless of catalyst loading or operating conditions. Plastic-to-liquid conversion rates of 75-92 wt% with calorific values of 43-46 MJ/kg, achieved at catalyst loadings 70-80% lower than conventional systems, indicate the technological feasibility of nano-catalytic pyrolysis as a method for circular economy integration of plastic waste.

However, this assessment also highlights three limits which the field has to address before industrial implementation is possible. First, catalyst deactivation by coking, sintering and, in mixed-plastic feeds, chlorine poisoning is still poorly understood; multi-cycle stability data beyond ten regeneration cycles are mostly missing in the literature. Second, life cycle and techno-economic assessments are few and inconsistent, making it impossible to assess if reactor-level energy savings survive comprehensive system accounting. Third, little consideration has been paid to the environmental and occupational health concerns of manufactured nanoparticles in industrial process environments in this application. Hence, future work should focus on three areas: (i) systematic deactivation studies with industrially relevant mixed-plastic feeds and with longer cycle counts; (ii) standardisation of techno-economic and LCA frameworks that allow cross-comparison of studies; and (iii) AI-enabled catalyst design to shorten the development time from years to months by learning structure-activity relationships from the expanding experimental data set. Progress in these fields will decide if nano-catalytic valorisation of plastic can be converted from a laboratory phenomenon to a cornerstone of the sustainable waste management infrastructure.

Acknowledgement:
We would like to show our gratitude to the our institute Vel Tech Rangarajan Dr. Sagunthala R&D Institute of Science and Technology, Chennai, India for providing resources for this review in successful manner. Also, the authors extend their appreciation to Universiti Teknikal Malaysia Melaka (UTeM) for their support in this research.

Author Contributions:
S. Padmanabhan contributed to the research concept and design, data analysis and interpretation, and writing of the article.
Jamil Abdelrahim Jamil Alsayaydeh contributed to the research concept and design, data analysis and interpretation, writing of the article, and final approval of the manuscript.
T. Vinod Kumar contributed to the collection and assembly of data and critical revision of the article.
S. Ganesan contributed to the data analysis and interpretation and critical revision of the article.
Rex Bacarra contributed to the collection and assembly of data and writing of the article.
Nadzrie Bin Mohamood contributed to the collection and assembly of data and critical revision of the article.

All authors reviewed and approved the final version of the manuscript.

Disclosure of interest:
The authors declare that they have no known competing financial interests or personal relationships that could have appeared to influence the work reported in this paper.
Declaration of funding:
The authors declare that No funding or sponsorship was receive for this work.
Data Availability:
Not applicable.
Clinical Trial Registration: *Not applicable.*
Consent to Publish: *Not applicable.*
Consent to Participate: *Not applicable.*
Ethics Approval: *Not applicable.*

References

1. Abbas-Abadi, M. S., Haghighi, M. N., Yeganeh, H., & McDonald, A. G. (2014). Evaluation of pyrolysis process parameters on polypropylene degradation products. Journal of Analytical and Applied Pyrolysis, 109, 272–277. https://doi.org/https://doi.org/10.1016/j.jaap.2014.05.023

2. Acomb, J. C., Wu, C., & Williams, P. T. (2016). The use of different metal catalysts for the simultaneous production of carbon nanotubes and hydrogen from pyrolysis of plastic feedstocks. Applied Catalysis B: Environmental, 180, 497–510. https://doi.org/https://doi.org/10.1016/j.apcatb.2015.06.054

3. Aguado, J., Serrano, D. P., San Miguel, G., Castro, M. C., & Madrid, S. (2007). Feedstock recycling of polyethylene in a two-step thermo-catalytic reaction system. Journal of Analytical and Applied Pyrolysis, 79(1), 415–423. https://doi.org/https://doi.org/10.1016/j.jaap.2006.11.008

4. Ahamed, A., Veksha, A., Yin, K., Weerachanchai, P., Giannis, A., & Lisak, G. (2020). Environmental impact assessment of converting flexible packaging plastic waste to pyrolysis oil and multi-walled carbon nanotubes. Journal of Hazardous Materials, 390, 121449. https://doi.org/https://doi.org/10.1016/j.jhazmat.2019.121449

5. Ali, M. F., & Siddiqui, M. N. (2005). Thermal and catalytic decomposition behavior of PVC mixed plastic waste with petroleum residue. Journal of Analytical and Applied Pyrolysis, 74(1), 282–289. https://doi.org/https://doi.org/10.1016/j.jaap.2004.12.010

6. Alreshidi, M. A., Yadav, K. K., Gacem, A., Padmanabhan, S., Ganesan, S., Guganathan, L., Saravanan, P., Thajudeen, K. Y., Fallatah, A. M., Ahmed, M. M., Aldosari, F. M., Shoba, G., Kavitha, C., Tamizhdurai, P., Subramani, A., & Kumaran, R. (2025). Nanocatalytic upcycling of plastic waste: Advances in selective conversion technologies for sustainable high-value products recovery. Results in Engineering, 28. https://doi.org/10.1016/j.rineng.2025.107042

7. Al-Salem, S. M., Lettieri, P., & Baeyens, J. (2009). Recycling and recovery routes of plastic solid waste (PSW): A review. Waste Management, 29(10), 2625–2643. https://doi.org/https://doi.org/10.1016/j.wasman.2009.06.004

8. Antelava, A., Damilos, S., Hafeez, S., Manos, G., Al-Salem, S. M., Sharma, B. K., Kohli, K., & Constantinou, A. (2019). Plastic Solid Waste (PSW) in the Context of Life Cycle Assessment (LCA) and Sustainable Management. Environmental Management, 64(2), 230–244. https://doi.org/10.1007/s00267-019-01178-3

9. Anuar Sharuddin, S. D., Abnisa, F., Wan Daud, W. M. A., & Aroua, M. K. (2016). A review on pyrolysis of plastic wastes. Energy Conversion and Management, 115, 308–326. https://doi.org/10.1016/j.enconman.2016.02.037

10. Anuar Sharuddin, S. D., Abnisa, F., Wan Daud, W. M. A., & Aroua, M. K. (2017). Energy recovery from pyrolysis of plastic waste: Study on non-recycled plastics (NRP) data as the real measure of plastic waste. Energy Conversion and Management, 148, 925–934. https://doi.org/https://doi.org/10.1016/j.enconman.2017.06.046

11. Azam, M. U., Afzal, W., & Graça, I. (2024). Advancing Plastic Recycling: A Review on the Synthesis and Applications of Hierarchical Zeolites in Waste Plastic Hydrocracking. In Catalysts (Vol. 14, Issue 7, p. 450). https://doi.org/10.3390/catal14070450

12. Bartholomew, C. H. (2001). Mechanisms of catalyst deactivation. Applied Catalysis A: General, 212(1), 17–60. https://doi.org/https://doi.org/10.1016/S0926-860X(00)00843-7

13. Broclawik, E., Załucka, J., Kozyra, P., Mitoraj, M., & Datka, J. (2011). Formaldehyde activation by Cu(I) and Ag(I) sites in ZSM-5: ETS-NOCV analysis of charge transfer processes. Catalysis Today, 169(1), 45–51. https://doi.org/https://doi.org/10.1016/j.cattod.2010.08.020

14. Czajczyńska, D., Anguilano, L., Ghazal, H., Krzyżyńska, R., Reynolds, A. J., Spencer, N., & Jouhara, H. (2017). Potential of pyrolysis processes in the waste management sector. Thermal Science and Engineering Progress, 3, 171–197. https://doi.org/https://doi.org/10.1016/j.tsep.2017.06.003

15. Das, S., Liang, C., & Dunn, J. B. (2022). Plastics to fuel or plastics: Life cycle assessment-based evaluation of different options for pyrolysis at end-of-life. Waste Management, 153, 81–88. https://doi.org/https://doi.org/10.1016/j.wasman.2022.08.015

16. Demirbas, A. (2004). Pyrolysis of municipal plastic wastes for recovery of gasoline-range hydrocarbons. Journal of Analytical and Applied Pyrolysis, 72(1), 97–102. https://doi.org/https://doi.org/10.1016/j.jaap.2004.03.001

17. Ding, W., Liang, J., & Anderson, L. L. (1997). Hydrocracking and Hydroisomerization of High-Density Polyethylene and Waste Plastic over Zeolite and Silica−Alumina-Supported Ni and Ni−Mo Sulfides. Energy & Fuels, 11(6), 1219–1224. https://doi.org/10.1021/ef970051q

18. Feng, R., Liu, S., Bai, P., Qiao, K., Wang, Y., Almegren, H., Rood, M., & Yan, Z. (2014). Preparation and Characterization of γ-Al2O3 with Rich Brønsted Acid Sites and Its Application in the Fluid Catalytic Cracking Process. The Journal of Physical Chemistry C, 118, 6226–6234. https://doi.org/10.1021/jp411405r

19. Gacem, A., Sambandam, P., Santhosh, S., Silambarasan, T., Saravanan, P., Bairavi, B., Mangesh, P. V. L., Yadav, K. K., Khalid, M., Alqhtani, H. A., Bin-Jumah, M., Subramani, A., Kavitha, C., & Tamizhdurai, P. (2025). Catalytic hydroprocessing of mixed plastic waste using Ni-Ce/ZSM-5: Performance and emission analysis of diesel blends across blending ratios. Energy Reports, 13, 1590–1607. https://doi.org/10.1016/j.egyr.2025.01.016

20. Geyer, R., Jambeck, J. R., & Law, K. L. (2026). Production, use, and fate of all plastics ever made. Science Advances, 3(7), e1700782. https://doi.org/10.1126/sciadv.1700782

21. Gomis, A., Siurana, A., & Valdés, F. (2007). Catalytic pyrolysis of LDPE over H-beta and HZSM-5 zeolites in dynamic conditions. Journal of Analytical and Applied Pyrolysis, 79, 433–442. https://doi.org/10.1016/j.jaap.2006.09.006

22. Gracida-Alvarez, U. R., Mitchell, M. K., Sacramento-Rivero, J. C., & Shonnard, D. R. (2018). Effect of Temperature and Vapor Residence Time on the Micropyrolysis Products of Waste High Density Polyethylene. Industrial & Engineering Chemistry Research, 57(6), 1912–1923. https://doi.org/10.1021/acs.iecr.7b04362

23. Hasan, M. M., Haque, R., Jahirul, M. I., & Rasul, M. G. (2025). Pyrolysis of plastic waste for sustainable energy Recovery: Technological advancements and environmental impacts. Energy Conversion and Management, 326, 119511. https://doi.org/https://doi.org/10.1016/j.enconman.2025.119511

24. Hashemi, M., Nguyen, K. T. Q., Robert, D. J., Zhang, G. K., Hosseinnejad, T., & Marney, D. (2026). Advanced pyrolysis methods for mixed plastic waste management: Enhanced char and gas yields. Journal of Analytical and Applied Pyrolysis, 193, 107360. https://doi.org/https://doi.org/10.1016/j.jaap.2025.107360

25. Hijazi, N., Bavykina, A., Yarulina, I., Shoinkhorova, T., Ramos-Fernandez, E. V, & Gascon, J. (2025). Chemical engineering of zeolites: alleviating transport limitations through hierarchical design and shaping. Chemical Society Reviews, 54(13), 6335–6384. https://doi.org/10.1039/D5CS00169B

26. Ishihara, Y., Nanbu, H., Ikemura, T., & Takesue, T. (1990). Catalytic decomposition of polyethylene using a tubular flow reactor system. Fuel, 69(8), 978–984. https://doi.org/https://doi.org/10.1016/0016-2361(90)90008-E

27. Kusenberg, M., Eschenbacher, A., Djokic, M. R., Zayoud, A., Ragaert, K., De Meester, S., & Van Geem, K. M. (2022). Opportunities and challenges for the application of post-consumer plastic waste pyrolysis oils as steam cracker feedstocks: To decontaminate or not to decontaminate? Waste Management, 138, 83–115. https://doi.org/https://doi.org/10.1016/j.wasman.2021.11.009

28. Lee, Y.-Y., Srinivaas, M., Li, I.-C., Kenharika, K., Pothu, R., Boddula, R., Al-Qahtani, N., Huang, B.-W., & Chang-Chien, C.-P. (2024). Enhancing Sustainable Energy Through Cutting-Edge Waste Biorefinery Technologies. In Reactions (Vol. 5, Issue 4, pp. 1101–1147). https://doi.org/10.3390/reactions5040059

29. Li, H., Aguirre-Villegas, H. A., Allen, R. D., Bai, X., Benson, C. H., Beckham, G. T., Bradshaw, S. L., Brown, J. L., Brown, R. C., Cecon, V. S., Curley, J. B., Curtzwiler, G. W., Dong, S., Gaddameedi, S., García, J. E., Hermans, I., Kim, M. S., Ma, J., Mark, L. O., … Huber, G. W. (2022). Expanding plastics recycling technologies: chemical aspects, technology status and challenges. Green Chemistry, 24(23), 8899–9002. https://doi.org/10.1039/D2GC02588D

30. Li, J., Liu, T., Palansooriya, K. N., Yu, D., Wan, G., Sun, L., Chang, S. X., & Wang, Y. (2025). Zeolite-catalytic pyrolysis of waste plastics: Machine learning prediction, interpretation, and optimization. Applied Energy, 382, 125258. https://doi.org/https://doi.org/10.1016/j.apenergy.2024.125258

31. Lopez, G., Artetxe, M., Amutio, M., Bilbao, J., & Olazar, M. (2017). Thermochemical routes for the valorization of waste polyolefinic plastics to produce fuels and chemicals. A review. Renewable and Sustainable Energy Reviews, 73, 346–368. https://doi.org/https://doi.org/10.1016/j.rser.2017.01.142

32. Luo, G., Suto, T., Yasu, S., & Kato, K. (2000). Catalytic degradation of high density polyethylene and polypropylene into liquid fuel in a powder-particle fluidized bed. Polymer Degradation and Stability, 70(1), 97–102. https://doi.org/https://doi.org/10.1016/S0141-3910(00)00095-1

33. Maqsood, T., Dai, J., Zhang, Y., Guang, M., & Li, B. (2021). Pyrolysis of plastic species: A review of resources and products. Journal of Analytical and Applied Pyrolysis, 159, 105295. https://doi.org/https://doi.org/10.1016/j.jaap.2021.105295

34. Mehta, J., Dilbaghi, N., Deep, A., Hai, F. I., Hassan, A. A., Kaushik, A., & Kumar, S. (2025). Plastic waste upcycling into carbon nanomaterials in circular economy: Synthesis, applications, and environmental aspects. Carbon, 234, 119969. https://doi.org/https://doi.org/10.1016/j.carbon.2024.119969

35. Miandad, R., Barakat, M. A., Aburiazaiza, A. S., Rehan, M., & Nizami, A. S. (2016). Catalytic pyrolysis of plastic waste: A review. Process Safety and Environmental Protection, 102, 822–838. https://doi.org/https://doi.org/10.1016/j.psep.2016.06.022

36. Miandad, R., Barakat, M. A., Rehan, M., Aburiazaiza, A. S., Ismail, I. M. I., & Nizami, A. S. (2017). Plastic waste to liquid oil through catalytic pyrolysis using natural and synthetic zeolite catalysts. Waste Management, 69, 66–78. https://doi.org/https://doi.org/10.1016/j.wasman.2017.08.032

37. Mollick, M., Cortazar, M., Santamaria, L., Fernandez, E., Artetxe, M., Olazar, M., & Lopez, G. (2025). Upcycling HDPE plastic into value-added products via γ-alumina catalyzed steam cracking in a fountain confined spouted bed. Journal of Environmental Chemical Engineering, 13(1), 115170. https://doi.org/https://doi.org/10.1016/j.jece.2024.115170

38. Muhammad, S., Abubakar, K., & Abubakar, H. (2026). Thermo-Catalytic Cracking of Used Engine Oil into Gasoline-Range Hydrocarbons Over Na/K/Ca-Promoted Fe_3O_4 Nanoparticles Supported on HZSM-5. Scholars Journal of Physics, Mathematics and Statistics, 13, 32–48. https://doi.org/10.36347/sjpms.2026.v13i01.005

39. Nanda, S., Reddy, S. N., Vo, D.-V. N., Sahoo, B. N., & Kozinski, J. A. (2018). Catalytic gasification of wheat straw in hot compressed (subcritical and supercritical) water for hydrogen production. Energy Science \& Engineering, 6(5), 448–459. https://doi.org/https://doi.org/10.1002/ese3.219

40. Nguyen, M. D., Tran, H.-V., Xu, S., & Lee, T. R. (2021). Fe3O4 Nanoparticles: Structures, Synthesis, Magnetic Properties, Surface Functionalization, and Emerging Applications. In Applied Sciences (Vol. 11, Issue 23, p. 11301). https://doi.org/10.3390/app112311301

41. Obeid, F., Zeaiter, J., Al-Muhtaseb, A. H., & Bouhadir, K. (2014). Thermo-catalytic pyrolysis of waste polyethylene bottles in a packed bed reactor with different bed materials and catalysts. Energy Conversion and Management, 85, 1–6. https://doi.org/https://doi.org/10.1016/j.enconman.2014.05.075

42. Onwudili, J. A., Insura, N., & Williams, P. T. (2009). Composition of products from the pyrolysis of polyethylene and polystyrene in a closed batch reactor: Effects of temperature and residence time. Journal of Analytical and Applied Pyrolysis, 86(2), 293–303. https://doi.org/https://doi.org/10.1016/j.jaap.2009.07.008

43. Panda, A. K., Singh, R. K., & Mishra, D. K. (2010). Thermolysis of waste plastics to liquid fuel: A suitable method for plastic waste management and manufacture of value added products—A world prospective. Renewable and Sustainable Energy Reviews, 14(1), 233–248. https://doi.org/https://doi.org/10.1016/j.rser.2009.07.005

44. Pandiangan, K. D., Sodha, V., Bandyopadhyay, M., Kolesnichenko, N. V, Natalya, N., & Snatenkova, Y. M. (n.d.). Synthesis and Characterization of ZSM-5 Catalyst at Different Temperatures Synthesis and Characterization of ZSM-5 Catalyst at Different Temperatures. https://doi.org/10.1088/1757-899X/214/1/012032

45. Qureshi, M. S., Oasmaa, A., Pihkola, H., Deviatkin, I., Tenhunen, A., Mannila, J., Minkkinen, H., Pohjakallio, M., & Laine-Ylijoki, J. (2020). Pyrolysis of plastic waste: Opportunities and challenges. Journal of Analytical and Applied Pyrolysis, 152, 104804. https://doi.org/https://doi.org/10.1016/j.jaap.2020.104804

46. Ratnasari, D. K., Nahil, M. A., & Williams, P. T. (2017). Catalytic pyrolysis of waste plastics using staged catalysis for production of gasoline range hydrocarbon oils. Journal of Analytical and Applied Pyrolysis, 124, 631–637. https://doi.org/https://doi.org/10.1016/j.jaap.2016.12.027

47. Rossi, L. M., Costa, N. J. S., Silva, F. P., & Wojcieszak, R. (2014). Magnetic nanomaterials in catalysis: advanced catalysts for magnetic separation and beyond. Green Chemistry, 16(6), 2906–2933. https://doi.org/10.1039/C4GC00164H

48. Sarker, M., & Rashid, M. M. (2013). Waste Plastics Mixture of Polystyrene and Polypropylene into Light Grade Fuel using Fe 2 O 3 Catalyst. https://api.semanticscholar.org/CorpusID:53407414

49. Serrano, D. P., Aguado, J., & Escola, J. M. (2012). Developing Advanced Catalysts for the Conversion of Polyolefinic Waste Plastics into Fuels and Chemicals. ACS Catalysis, 2(9), 1924–1941. https://doi.org/10.1021/cs3003403

50. Serrano, D. P., Aguado, J., Escola, J. M., & Garagorri, E. (2003). Performance of a continuous screw kiln reactor for the thermal and catalytic conversion of polyethylene–lubricating oil base mixtures. Applied Catalysis B: Environmental, 44(2), 95–105. https://doi.org/https://doi.org/10.1016/S0926-3373(03)00024-9

51. Sharuddin, S. D. A., Abnisa, F., Daud, W. M. A. W., & Aroua, M. K. (2018). Pyrolysis of plastic waste for liquid fuel production as prospective energy resource. IOP Conference Series: Materials Science and Engineering, 334(1), 12001. https://doi.org/10.1088/1757-899X/334/1/012001

52. Shi, Y., Diao, X., Ji, N., Ding, H., Ya, Z., Xu, D., Wei, R., Cao, K., & Zhang, S. (2025). Advances and Challenges for Catalytic Recycling and Upgrading of Real-World Mixed Plastic Waste. ACS Catalysis, 15(2), 841–868. https://doi.org/10.1021/acscatal.4c06344

53. Singh, R. K., Ruj, B., Sadhukhan, A. K., & Gupta, P. (2019). Impact of fast and slow pyrolysis on the degradation of mixed plastic waste: Product yield analysis and their characterization. Journal of the Energy Institute, 92(6), 1647–1657. https://doi.org/https://doi.org/10.1016/j.joei.2019.01.009

54. Tang, Z., Chen, W., Chen, Y., Yang, H., & Chen, H. (2019). Co-pyrolysis of microalgae and plastic: Characteristics and interaction effects. Bioresource Technology, 274, 145–152. https://doi.org/https://doi.org/10.1016/j.biortech.2018.11.083

55. Undri, A., Rosi, L., Frediani, M., & Frediani, P. (2014). Efficient disposal of waste polyolefins through microwave assisted pyrolysis. Fuel, 116, 662–671. https://doi.org/https://doi.org/10.1016/j.fuel.2013.08.037

56. Verma, R., Singh, S., Dalai, M. K., Saravanan, M., Agrawal, V. V, & Srivastava, A. K. (2017). Photocatalytic degradation of polypropylene film using TiO2-based nanomaterials under solar irradiation. Materials & Design, 133, 10–18. https://doi.org/https://doi.org/10.1016/j.matdes.2017.07.042

57. Wang, W., Yao, S., Deng, S., Wang, Y., Qiu, C., Mao, C., & Wang, J. (2021). Sintering Rate and Mechanism of Supported Pt Nanoparticles by Multiscale Simulation. Langmuir, 37(43), 12529–12538. https://doi.org/10.1021/acs.langmuir.1c01628

58. Wei, L., Wang, H., Dong, Q., Li, Y., & Xiang, H. (2025). A Review on the Research Progress of Zeolite Catalysts for Heavy Oil Cracking. In Catalysts (Vol. 15, Issue 4, p. 401). https://doi.org/10.3390/catal15040401

59. Williams, P. T., & Slaney, E. (2007). Analysis of products from the pyrolysis and liquefaction of single plastics and waste plastic mixtures. Resources, Conservation and Recycling, 51(4), 754–769. https://doi.org/https://doi.org/10.1016/j.resconrec.2006.12.002

60. Yahaya, R., Brydson, R., Comyn, T., Scott, A., Hammond, C., Brown, A., Chauruka, S., Hassanpour, A., Young, N., Kirkland, A., Sawada, H., & Smith, R. (2013). A Study of Commercial Nanoparticulate -Al2O3 Catalyst Supports. ChemCatChem, 5. https://doi.org/10.1002/cctc.201200880

61. Yao, D., Yang, H., Chen, H., & Williams, P. T. (2018). Co-precipitation, impregnation and so-gel preparation of Ni catalysts for pyrolysis-catalytic steam reforming of waste plastics. Applied Catalysis B: Environmental, 239, 565–577. https://doi.org/https://doi.org/10.1016/j.apcatb.2018.07.075

62. Zhang, X., Lei, H., Chen, S., & Wu, J. (2016). Catalytic co-pyrolysis of lignocellulosic biomass with polymers: a critical review. Green Chemistry, 18(15), 4145–4169. https://doi.org/10.1039/C6GC00911E